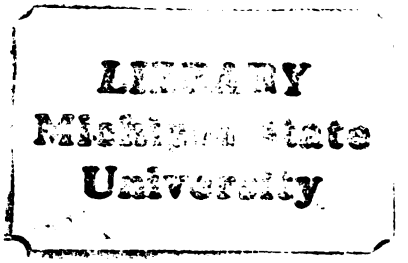

This is to certify that the

thesis entitled

The Effect of Elbow Restraint on
Pressure Transients

presented by

Robert Stephen Otwell

has been accepted towards fulfillment
of the requirements for

Doctoral degree in Civil Engineering

David Wyjgert
Major professor

Date 11 May 84

THE EFFECT OF ELBOW RESTRAINT ON PRESSURE TRANSIENTS

By

Robert Stephen Otwell

A DISSERTATION

Submitted to
Michigan State University
in partial fulfillment of the requirements
for the degree of

DOCTOR OF PHILOSOPHY

Department of Civil and Sanitary Engineering

1984

ABSTRACT

THE EFFECT OF ELBOW RESTRAINT ON PRESSURE TRANSIENTS

By

Robert Stephen Otwell

Transient pressure in piped liquid is a function of structural restraint at an elbow. When supported rigidly, the elbow causes no appreciable alteration of the pressure transient generated by rapid valve closure. However, if the support is relaxed, significant pressure alteration is observed, with peak pressures being greater than the traditional Joukowsky pressure rise. Elbow motion, driven by the axial stresses in the pipe and the fluid pressure, causes the alteration.

A numerical model is developed and verified with experimental data. The one-dimensional equations of continuity and momentum for the liquid and pipe wall are solved by the method of characteristics. At an elbow, coupling is introduced by continuity relationships. The translation of attached piping at an elbow is represented by

an added stiffness term, and solved simultaneously with the characteristic equations. Comparison is shown between experimental data and predicted results. The equations are normalized and dimensionless parameters are identified that describe the liquid-pipe interaction.

ACKNOWLEDGMENTS

The author wishes to express his gratitude to the members of his doctoral committee for their assistance; Reinier Boumeester, Merle Potter, and Sidney Stuckenbruck. In particular, the author wishes to thank David Wiggert, chairman of the committee, under whose advice and supervision the work was carried out, and committee member Frank Hatfield, for his encouragement and guidance throughout the work.

The author is indebted to the Department of Civil and Sanitary Engineering for teaching and research assistantships, and to the National Science Foundation for their financial support.

The author also wishes to thank his sister Carol for help in preparation of the manuscript, and his wife Laura for her interest and encouragement during the project.

TABLE OF CONTENTS

LIST OF TABLES

LIST OF FIGURES

LIST OF FIGURES (cont'd)

NOMENCLATURE

a	Wavespeed in infinite medium, m/s
A	Cross-sectional area, m^2
A1,A2	Coefficient matrices
C_f	Liquid wavespeed in pipe, m/s
C_t	Pipe axial wavespeed, m/s
C+,C-	Characteristic lines
e	Pipe wall thickness, m
E	Young's modulus of elasticity, Pa
E^*	$E/(1-\nu^2)$, Pa
H	Dimensionless parameter (equation 23)
J	Dimensionless parameter (equation 15)
K	Bulk modulus of liquid, Pa
K	Stiffness coefficient, N/m
L	Pipe length, m
p	Pressure, Pa
Q1,Q2	Dimensionless parameters (equations 22, 23)
r	Pipe radius, m
R	Elbow radius, m
S	Constant relating initial flow and pressure
t	Time, s
T	Transformation matrix
u	Pipe axial displacement, m

NOMENCLATURE (cont'd)

$\dot{u}$	Pipe axial velocity, m/s
V	Liquid velocity, m/s
V_r	Relative velocity, m/s
w	Pipe radial displacement, m
W	Dimensionless parameter (equations 14 and 16)
x	Distance along pipe axis, m
Z	Matrix of dependent variables
ε	Strain
λ	Characteristic roots
ν	Poisson ratio
ρ	Density, kg/m^3
σ	Stress, Pa
τ	Dimensionless valve opening

Subscripts

f	Liquid
t	Pipe
x	x-direction
y	y-direction
θ	Circumferential direction

Chapter 1

INTRODUCTION

1.1 Problem Introduction

Piping systems used for transfer of pressurized liquids operate under time varying conditions imposed by pump and valve operation. Unsteady pressures and flows result, which are known as liquid transients, waterhammer, or surges. Traditionally, to analyze the unsteady behavior of the liquid, the equations of motion and continuity of the liquid are solved without regard to the motion of the piping. The transients propagate at the acoustic velocity, or wavespeed, of the liquid in the pipe. The diameter, wall thickness, and elastic modulus of the piping are used in computing the wavespeed, after which the liquid is assumed to be flowing through a straight, rigid pipe.

Recently there has been concern that the transient behavior of liquid in a piping system that is neither rigid nor straight may differ from that predicted by a traditional rigid pipe analysis. It is reasoned that the dynamic forces exerted by the liquid at fittings (elbows, tees, valves, and

reducers) where flow direction or area changes can set the pipe in motion and the feedback between the liquid and pipe can cause alteration of the liquid behavior. Some investigators have suggested that this alteration is either negligible or that a rigid pipe analysis would provide a conservative estimate of the transient pressure because of the transfer of energy out of the liquid and into the structure. However, experiments have shown that in some systems, the response of the piping amplifies transient pressure in the liquid.

Motion of fittings is caused by dynamic forces in the liquid and pipe wall. The amplitude and velocity of motion are functions of the restraint provided by the attached piping and supports. It is apparent that the analysis of liquid in a piping system must include information on the piping structure itself. A coupled liquid-pipe analysis must consider structural parameters.

1.2 Background

In the late 1800's Joukowsky [1] determined that the wavespeed of liquid in a pipe, and hence the speed at which liquid discontinuities propagate, was related to the relative circumferential stiffness of the pipe. This wavespeed is an "apparent" wavespeed and is less than the true wave propagation speed in an infinite liquid.

Joukowsky assumed that pressure is uniform across any cross section and that the radial dilation of the pipe is equal to the static dilation that would be caused by the pressure. That is, he neglected the radial inertia of the liquid, mass of the pipe wall, and axial and bending stresses in the wall.

Since Joukowsky's time, much work has been done on liquid transients in piping systems. Works by Wylie and Streeter [2], and Chaudhry [3] outline analytical techniques to solve many types of problems with various boundary conditions. The remaining literature review will concentrate on liquid-pipe interaction.

Contained liquid interacts with piping in several ways: internal pressure causes circumferential strain of the pipe wall; pressure resultants act at locations where flow direction or area change; high steady flow rates induce lateral pipe motion; and, the transverse acoustic modes in the liquid may interact with shell modes of the pipe wall. This thesis will only consider two mechanisms of dynamic interaction between the contained liquid and the piping: 1) strain-related effects which occur axially along pipe reaches; and 2) pressure resultant effects, where coupling occurs only at fittings.

1.2.1 Strain-related coupling

Strain-related or Poisson coupling results from the transformation of circumferential strain caused by internal pressure to axial strain due to Poisson's ratio:

$$\varepsilon_x = \nu \, \varepsilon_\theta \qquad (1)$$

Where ε_x and ε_θ are axial and circumferential strain and ν is Poisson's ratio.

Skalak [4] extended Joukowsky's method to include Poisson effects. The extension consisted of treating the pipe wall as an elastic membrane to include the axial stresses and axial inertia of the pipe. For sudden valve closure, an axial tension wave was found to propagate in the pipe wall at a wavespeed near that of the pipe material, hence a "precursor" wave travels ahead of the main pressure wave in the liquid. The axial tension is a Poisson effect in response to pipe dilation caused by the pressure transient. An increase in liquid pressure due to the tension wave was identified, but this increase was small because it was caused by the contraction in pipe diameter due to the tension wave; it is a second order Poisson effect. Thorley [5] completed a study very similar to Skalak's, including experimental validation of the theory. Williams [6] also conducted a similar study and found that the longitudinal and flexural motion caused damping that was greater than the

viscous damping in the liquid. The researchers discussed did not include the radial inertia of the liquid or pipe wall. Comments were made on damping due to radial motion as the wave traveled through the pipe and the damping was found to be small.

Walker and Phillips [7] proposed a new theory that included the radial inertia of the pipe wall because they were interested in transients of very short duration. They formulated a one-dimensional, axisymmetric system of six equations that included the radial and axial equations of motion of the pipe wall, two constitutive equations for the pipe wall, and the equation of motion and continuity for the liquid. They reported that the method "retains much of the rigor of the axisymmetric, two-dimensional approach" of Lin and Morgan [8]. They found their method is ideal for transients where the generation of the pressure pulse occurs in several microseconds, and that the classical waterhammer equations are adequate for longer pulse lengths.

The researchers discussed identified two important waves in a straight length of pipe, one in the pipe wall and one in the liquid, and they identified interaction between the liquid and pipe. None of these studies considered the possibility that a fitting, such as an elbow, might move in response to the precursor wave and alter the transient response of the liquid.

1.2.2 Pressure Resultants

At fittings where the pipe area or direction changes, the pressure resultant acts as a localized force on the pipe. The discussion of past research concerning pressure resultants will first consider periodic liquid forces, then non-periodic forces.

1.2.2.1 Periodic Forces

Blade, Lewis, and Goodykoontz [9] in 1962 were among the first to report on the alteration of the liquid behavior due to the motion of an elbow. They studied harmonic loading on a single elbow and reported the elbow provided coupling between the pipe and liquid but caused no appreciable reflection or attenuation. Wood [10] also studied harmonic loading of a pipe structure analytically by representing the structure as a single degree of freedom spring-mass. He found that the natural frequencies of the liquid were shifted, especially when the frequency of the loading was near one of the natural frequencies of the supporting structure.

Davidson and Smith [11], interested in the generation of noise due to harmonic loadings from pumps, developed an eight-equation system to solve for the eight degrees of freedom in the plane of a single elbow. The eight degrees of freedom consisted of an axial and radial pipe displacement, an axial liquid displacement, and a rotation,

at each end of the elbow. An experimental setup verified the theory. In a later paper, Davidson and Samsury [12] studied a more complex system with three elbows connected by short straight lengths. In both studies they identified significant coupling between the pressure waves in the fluid and the pipe.

Hatfield, Wiggert, and Otwell [13] developed a general solution procedure to study fluid-pipe interaction with harmonic loadings. The eigen solution of the supporting pipe structure is obtained from an existing finite element structural program. The modal responses are then coupled to the liquid analyses by a method known as component synthesis. This method was validated experimentally in a follow-up paper [14].

Phillips [15] studied the reflection and transmission of harmonic liquid loads at elbows by coupling the liquid and pipe equations. He found reflection and transmission coefficients of about 15% and 85%, respectively, for sharp and gentle bends for a frequency range of 100-10,000 hz. At higher frequencies no alteration was found. The model accounted for bending, shear and axial forces in the pipe, axial displacements, and liquid pressures. No comment was made as to the reason for the alteration around the elbows.

1.2.2.2 Non-periodic Forces

This dissertation will concentrate on the alteration of the liquid behavior due to non-periodic forces. The following is a review of the literature for that class of problem. Wood [16] investigated the effect of pipe motion on the pressure generated by rapid valve closure. He studied analytically and experimentally the effect of structural motion on the liquid behavior as a function of structural parameters and valve closure rate. His experiment involved a straight pipe with a pressure tank upstream and a simply-supported beam connected to a slip ring at the other end, with a branch and valve immediately upstream of the beam. The valve was slammed and the pressure resultant forces set the beam in motion. It was concluded that the beam response could significantly alter pressures.

Wood and Chao [17] set up an experimental apparatus that included an elbow between two 6 m lengths of copper pipe, with a quick closing valve downstream and a constant pressure reservoir upstream. Results were obtained with the elbow restrained by a supporting structure and with the elbow unrestrained. For the restrained case the pressure rise resembled the traditional Joukowsky prediction. For the unrestrained case, there was alteration of the pressure response in the form of a oscillation about the pressure observed for the restrained case. This alteration was

thought to be caused by motion of the elbow driven first by a stress wave in the pipe and then by the pressure wave. An analytical method was devised that used the measured structural velocities from the experiment as input into flow conservation relationships at the elbow in the liquid model. Favorable comparisons were shown between this analysis and the experiment.

Ellis [18] developed an analytical procedure to couple liquid equations with the equations for axial motion of piping. Coupling took place at fittings such as valves, elbows and branches, and mass and stiffness were lumped at the fittings. The Poisson effect was not included in the analysis.

Schwirian and Karabin [19], Giesecke [20], Otwell [21], and Wiggert and Hatfield [22] all developed general analytical techniques to couple liquid and pipe equations in order to study the dynamics of general piping systems. In all these studies, coupling was imposed only at fittings, and the effect of support and piping stiffness was shown to be significant.

In contrast, Swaffield [23] found that the influence of an elbow on liquid behavior was solely dependent on its dimensions: radius of curvature to pipe diameter ratio and included angle. He experimentally determined reflection and transmission coefficients of 20% and 80% respectively. Pipeline restraint was found to have no effect.

1.3 Scope

It is apparent that although there is much evidence suggesting that the behavior of liquid in piping can be influenced by the piping system that contains it, the actual mechanisms governing the alteration are not fully understood. Two types of coupling have been identified but their significance and their relationship to each other have not been quantified. The studies related to Poisson effects dealt only with straight pipes. At pipe fittings, pressure resultant forces have been shown to be important in vibrating piping; typical methods of solution include coupling only at fittings, ignoring the Poisson effect. Little experimental validation has been attempted.

The main objective of this study was to design and build an experiment that isolated the important parameters of liquid-pipe interaction. Structural restraint of an elbow was the independent variable. Very stiff supports were used for the control case of an immobile elbow. An elbow restrained only by the axial stiffnesses of the connecting pipes was studied so that the Poisson effect could be observed. Elbows restrained by the flexural stiffness of short pipe lengths were studied to observe a more flexible system.

A numerical model was developed that incorporates structural parameters necessary to represent the coupling mechanisms. The model simplifies the six-equation Walker and Phillips [7] development by ignoring the radial inertia term. The resulting equations are easily implemented in a numerical solution procedure. At an elbow, coupling is introduced by continuity relationships and the translation of attached piping can be represented by an added stiffness term. Comparisons are shown between predicted responses and experimental data for different restraint conditions.

Chapter 2 presents the design of the experiment and results. Chapter 3 contains the theoretical development, and Chapter 4 the numerical formulation, comparison with experimental results and an investigation into the important parameters involved in liquid-pipe interaction. Chapter 5 provides a summary discussion and conclusions.

Chapter 2

EXPERIMENT

2.1 Experimental Setup

2.1.1 Motivation

The purpose of the experiment was to enable observation of the alteration of a generated pressure transient for varied structural restraints at an elbow. From this the important pipe parameters influencing the alteration could be determined. One extreme was to fix the elbow rigidly and determine if geometric aspects of the elbow caused significant alteration of the liquid behavior. Once that was established, the alteration of the liquid behavior as a function of the structural restraint could be determined.

Before discussing the copper pipe experiment and results, a previous experiment using polyethylene pipe will be discussed. Many of the design considerations incorporated in the copper pipe experiment were a result of knowledge gained from the original experiment. The original experiment was designed to isolate a single elbow. Polyethylene pipe was used because of its high flexibility.

The flexibility was desired for two reasons: 1) the elbow restraint depended on pipe properties only to a small degree; and 2) the liquid wavespeed would be low and the vibrations could be observed before reflections from boundaries returned to the elbow. The pipe was wrapped on a circular (radius 2.5 m) frame. At the middle of the length, the pipe came off the frame and was straight for 3 m to a 90 degree elbow. Then another 3 m straight pipe came back to the frame.

Problems resulted from the mounting system; the frame itself moved as the transient traveled through the pipe. This was not anticipated as the 2.5 m radius was chosen to minimize the pressure resultant forces. Also there was a gradual rise in the pressure response at the valve, along with vibrations of the valve itself, which made observing the structural effects attributable to the elbow very difficult.

The objective was to mount supports with different stiffnesses at the elbow to create varied structural restraint. The first case considered was one without any support at the elbow. The elbow and attached piping were suspended by wire supports. It was expected that the elbow would move in the direction of the resultant pressure when the pressure transient from slamming the valve traveled upstream to the elbow. However, the initial direction of movement was parallel to the downstream pipe leg and in the

direction of shortening the leg. This was determined to be from the precursor tension wave which pulled the elbow before the pressure wave arrived. This observation, although puzzling at first, turned out to be the major motivation for the bulk of the remaining dissertation, including the design of the copper pipe experiment and a more thorough search of the literature on the precursor wave leading to an analytical method incorporating both the precursor and pressure resultant effects.

2.1.2 Pipe and Liquid Parameters

This section discusses the different parameters considered in the design of the pipe experiment. Since the experiment was designed to vary the restraint of the pipe, and not the type of pipe or contained liquid, many of the parameters were constants throughout the experiments.

The pipe parameters are:

ρ_t-density
E-Young's modulus
ν -Poisson's ratio
r -inside radius
e -wall thickness
R -elbow radius
σ_x-axial stress
$\dot{u}$ -axial velocity
w -radial displacement

The experiment consisted of a piping layout using 1 inch copper pipe with standard fittings. Because of that, ρ_t, E, ν, r, e, and R were all fixed and could not be varied. Axial velocity and axial stress were the important variables

to study. The axial velocity and axial stress are dependent on the restraint imposed on an elbow. The axial velocity was measured at the elbow with accelerometers. The radial displacement of the pipe is a function of the internal pressure and was not restrained.

The liquid parameters are:

ρ_f-density
K -bulk modulus
C_f-wavespeed
p -pressure
V -axial velocity

The mean density and bulk modulus remained constant. Water was the contained liquid. The liquid wavespeed was determined by measuring the time delay between two pressure transducers at a known distance apart. The liquid wavespeed was found to be 1270 m/s. The dynamic pressure was the important dependent liquid variable. The pressure was monitored by pressure transducers at several locations. The steady-state liquid velocity was controlled by varying the mean pressure drop between two pressure tanks.

During the experiments, environmental temperature and humidity were monitored. Their variations were found to be too small to affect significantly the observed pressures and accelerations.

2.1.3 Design Considerations

Certain variables must be controlled during the experiments. To do this, the design incorporates the following constraints:

2.1.3.1 Piping

The valve and piping outside the reach to be investigated must be rigidly supported in all directions. The reach to be investigated needs to be supported, ideally by supports that contribute negligible stiffness, inertia and damping for motion in the plane of the elbow. The lengths of pipe upstream of the elbow must be long enough to permit observation of the elbow's vibration before the reflection returns from the upstream end. Two elbows are incorporated so that a combination of restraints is possible, including one that allows translation of a section of pipe between the elbows.

2.1.3.2 Liquid

The liquid flow is controlled at the upstream and downstream ends of the pipe. The upstream end is a constant pressure tank and the downstream end is a valve connected to another pressure tank. The valve closes rapidly to cause an abrupt pressure rise so that the Poisson effects and pressure resultant effects on the elbow can be differentiated. The

valve closes in a time period such that the sum of the valve closure time plus the tension wave travel time to the elbow is less than the pressure wave travel time from the valve to the elbow. This will ensure that the full Poisson effect will take place before the pressure wave begins arriving. The generated pressure transient is a function of the steady-state flow velocity V_0, so there must be control of the steady-state pressure drop across the system to control the velocity.

2.1.4 Pipe Setup

Figure 1 is a schematic of the pipe setup. There is a total of 47.9 meters of 1 inch (nominal) diameter copper pipe between the upstream pressure tank and the valve. The pipe material constants (obtained from the manufacturer) are: ρ_t=8940 kg/m^3, E=117 GPa, ν=0.34, r=13 mm and e=1.27 mm. The system has a total of six elbows, with R=20.6 mm. The elbow to be studied is elbow 1. Rigid connections anchored to concrete walls or floor are used at elbows 3, 4 and 5, and as needed for elbows 1 and 2, depending on the restraint desired. The two main test sections of copper pipe (L1 and L2) are suspended by wire hangers to allow movement in the plane of elbow 1 and to keep the pipe from sagging and hence changing the axial stiffness characteristics. Where necessary, the pipes are hung within wooden enclosures for protection.

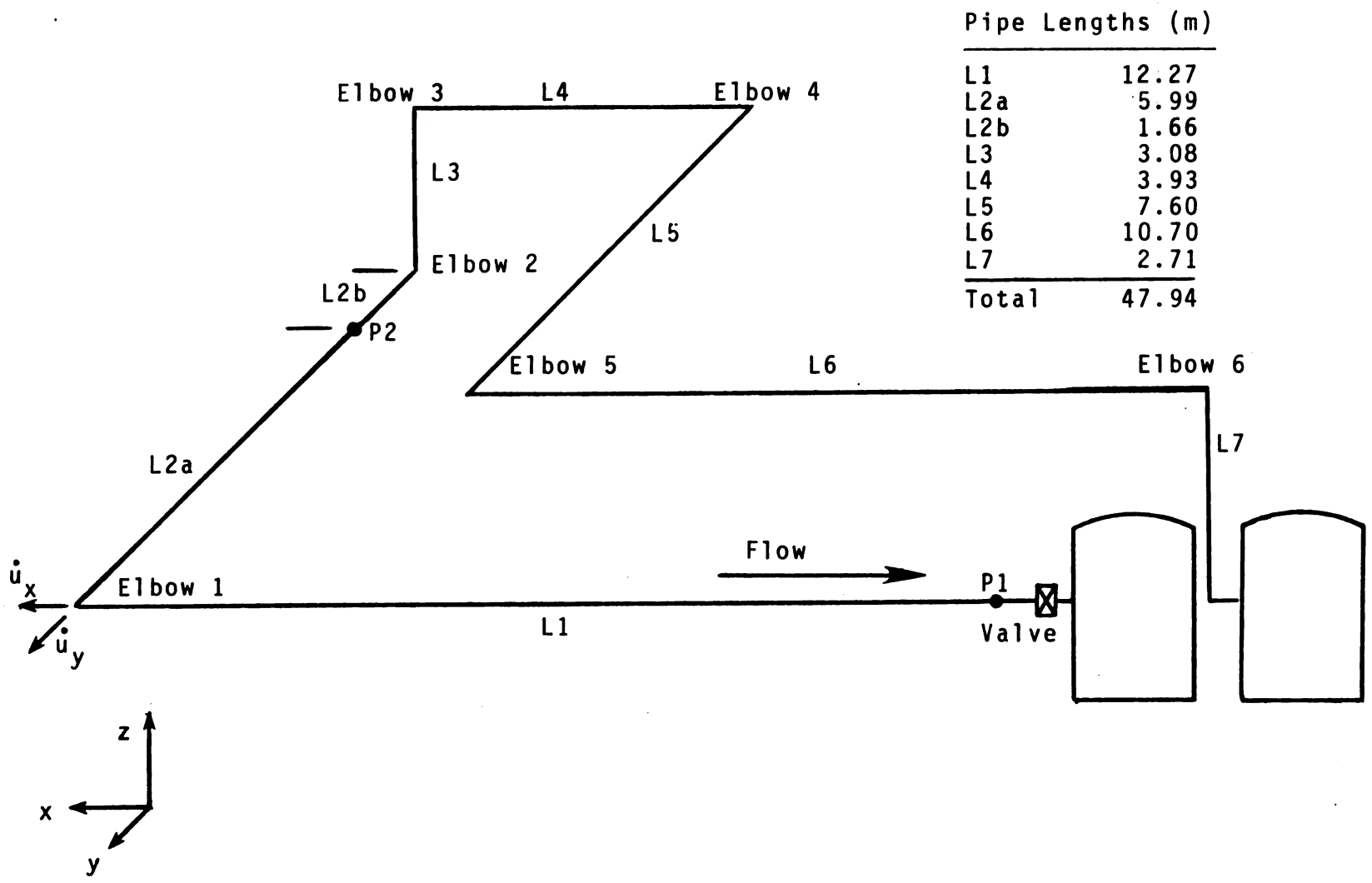

Figure 1. Schematic of Experimental Setup

The valve is a critical part of the setup as it has to close very quickly. The design of the valve is similar to one used by Wood [17]. As shown in Figure 2, the valve consists of an inlet chamber with an orifice connected to another chamber in the main valve block with an outlet 90 degrees from the inlet. The orifice has a hard rubber washer glued on the upstream side. The two pieces of the valve body are joined by four bolts and sealed with an O-ring. Running through the orifice and out the end of the block is a brass rod that enlarges to a diamond shape in front of the orifice and a ball outside the block. Where the rod goes through the block there is a Teflon sleeve. Operation of the valve is manual: the rod is pulled through the valve, and as the diamond-shaped seat approaches the orifice, differential pressure develops and slams the seat against the rubber washer. The valve has a closure time of approximately 4 ms. The valve body itself is bolted to the floor with two bolts and threaded expansion anchors (Figure 3). The valve closure, though hand actuated, has been found to be repeatable.

The rigid supports (Figure 4) are designed to resist axial pipe motion. The supports are made from aluminum blocks. In each block a hole was drilled to a diameter equal to the outside diameter of the pipe and then cut at the centerline of the hole. The cut removed 1 mm of material. The pipe is held in place by bolting the upper and lower pieces of the block together. The supports are then bolted to the floor.

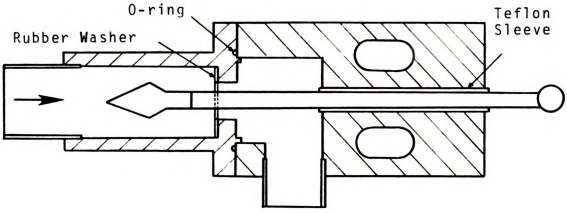

Figure 2. Valve (Top View)

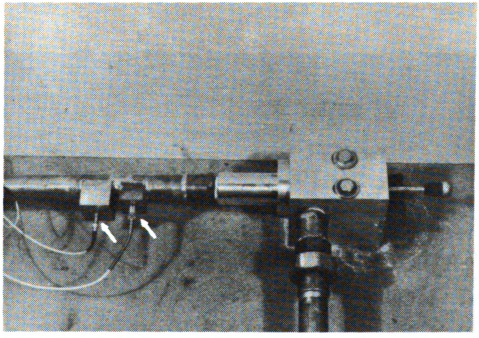

Figure 3. Pressure Transducers and Valve

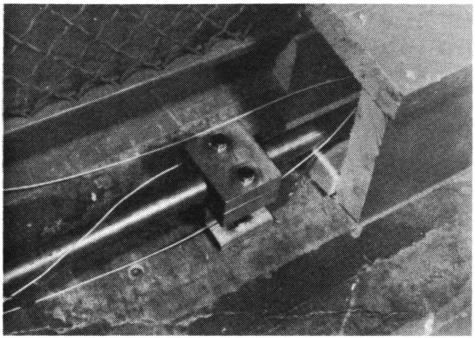

Figure 4. Stiff Support

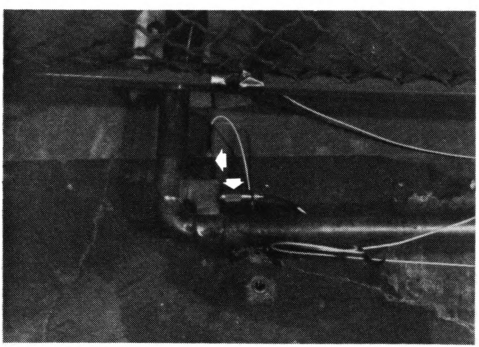

Figure 5. Elbow and Accelerometers

An air purge is located just upstream of elbow 4, the highest elevation on the piping system. This consists of a short, small diameter copper tube with a valve soldered to the copper pipe. Air can be bled off when the system is under pressure.

2.1.5 Data Acquisition

To obtain information on the behavior of the experimental setup, dependent variables must be recorded as a function of time. This is accomplished by measuring pressure and acceleration with transducers. The transducer converts the pressure or acceleration to voltage which is amplified and transferred to a recording device. Data were obtained on pressure at two locations, and on acceleration in orthogonal directions at one location. The information then could either be viewed on a storage oscilloscope or recorded on a digital computer.

2.1.5.1 Pressure Transducers

PCB Piezotronics Model 111A26 quartz pressure transducers were used to measure the dynamic pressure at two locations (P1 and P2) as shown on Figure 1. These transducers were chosen because of their high frequency response and because they are acceleration compensated. Between the transducers and recording device was a PCB Model 480D06 battery power unit. The transducers were mounted by tapping a brass block

per PCB specifications and then soldering it to the pipe. The hole was drilled so the tip of the transducer would mount flush with the inside of the pipe. One Sensotec Model "S" strain gage type pressure transducer was mounted at the valve for preliminary setup and testing. This transducer measured the static and dynamic pressure. It was also used as a trigger for the recording devices. The PCB (left) and Sensotec (right) transducers are shown in Figure 3.

2.1.5.2 Accelerometers

PCB Model 302A quartz accelerometers were used to measure the movement of elbow 1. The accelerometers were mounted on a brass block that was soldered to the inside of the elbow (Figure 5). Between the transducer and recording device was a PCB Model 480A08 integrating power unit. It could be switched to output either the acceleration or velocity by electronic integration.

2.1.5.3 Analog to Digital Conversion

Data were recorded and stored by a Digital Equipment Corporation (DEC) PDP-11/02 mini-computer. Transducer voltages were run through an A/D converter and stored as digital quantities. The hardware includes a DEC Model ADV11-C A/D converter and a DEC Model KWV11-C real-time clock. Software was developed to control the A/D converter and clock. A FORTRAN control program CONTRL (listing in

Appendix) drives an assembly language sampling subroutine SAMPL (listing in Appendix). Input data into CONTRL consist of the sampling rate, number of samples, and the channels to sample. The sampling begins with activation of a Schmitt trigger by the Sensotec transducer. SAMPL is an interrupt driven, clocked sampling subroutine that can take samples at a maximum rate of 10 kHz on one channel. The samples are stored in an array, then transferred back to CONTRL to be converted to pressure and velocity units and stored on a floppy disk to be printed or plotted. A Tektronix Model 5103N oscilloscope was used for visual monitoring of the transducers.

2.2 Experimental Results

2.2.1 Introduction

The following sections contain the results obtained from four different restraint conditions. The results consist of the pressure response at P1 (the valve) and at P2, and the axial velocities of elbow 1 for various structural restraints. Figure 6 shows the configurations for the four cases. From elbow 3 upstream to the pressure tank the system is the same for all cases.

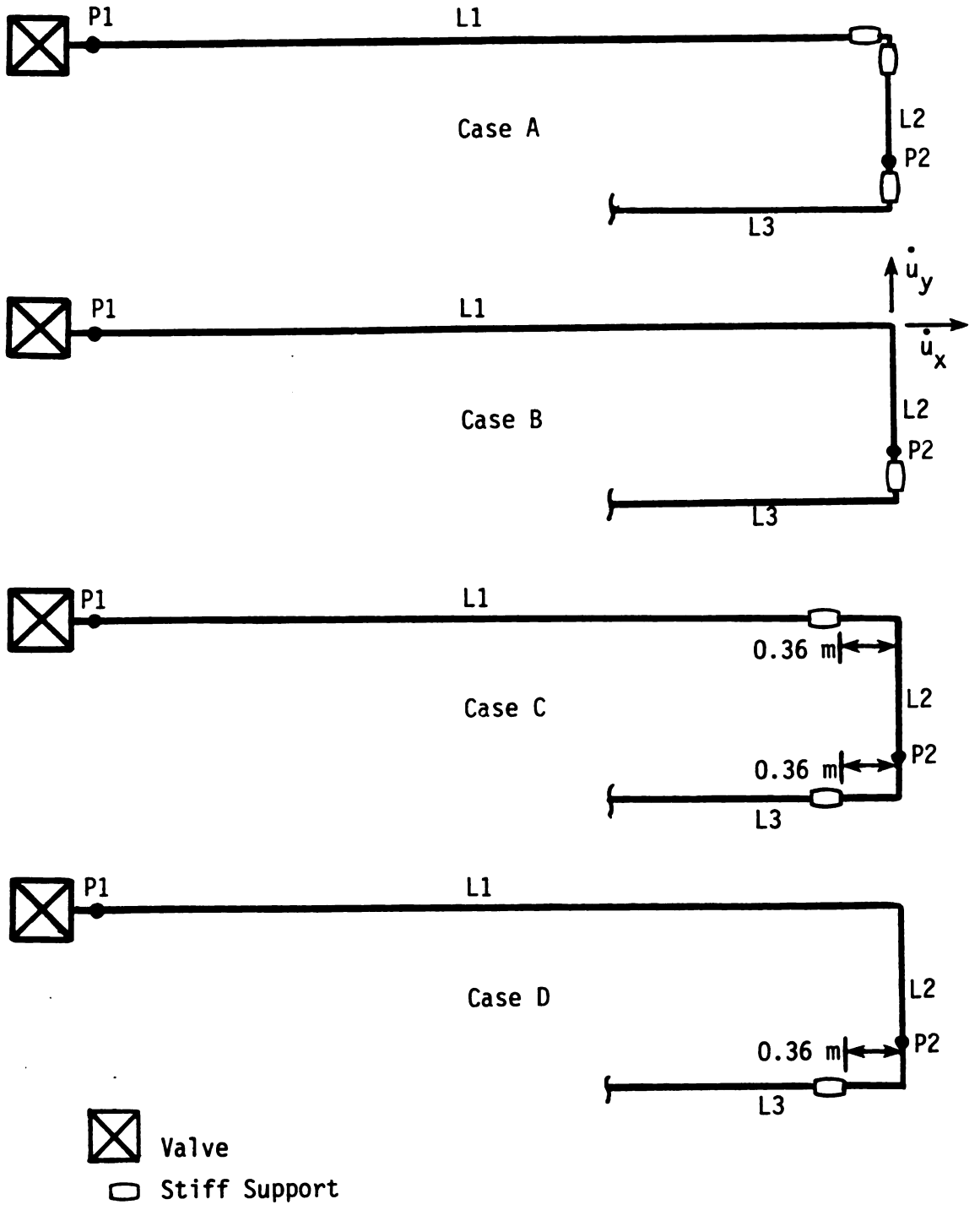

Figure 6. Structural Restraint for Four Experimental Setups

The first setup, Case A, has all the elbows supported rigidly in all directions. For the second setup, Case B, the stiff supports were removed at elbow 1 so that it is restrained by the axial stiffnesses of legs L1 and L2. The third setup, Case C, has two stiff supports placed 0.36 m from elbows 1 and 2. Axial translation of leg L2 is restrained by the bending stiffness of the two short lengths. This arrangement is less stiff than Case B because pipes are much stiffer axially than in flexure. The fourth setup, Case D, represents a combination of Case B and Case C. The final setup discussed, Case E, is the stiff system (Case A) with the support at the valve removed to observe liquid-pipe interaction caused by a fitting other than an elbow.

2.2.2 Case A: Stiff System

Figure 7 shows the pressure response at locations P1 and P2 for the stiff system. The interval of the pressure rise at P1 (hence the valve closure time) is approximately 4 ms. On subsequent plots, the data acquisition process will be triggered by the Sensotec transducer at the valve. Therefore, the initial 2 ms of pressure rise will not show at P1.

A common assumption of one-dimensional transient analysis procedures is that there is no alteration of the liquid transient behavior as it travels around a bend. The

experiment was designed so that this assumption could be verified on a system with a truly fixed elbow, which was the reason for placing the two stiff supports at elbow 1, the main test elbow.

Figure 8 shows the responses triggered by the transducer which can be used for comparison with the experiments to be described later. The sampling frequencies for Figures 7 and 8 are 1 kHz and 2 kHz, respectively. The higher sampling frequency shows a pressure spike due to flutter as the valve seats against the rubber washer. The pressure spike does not affect the subsequent pipe response. The remaining transducer data for Case B through Case F shown on Figures 9-12 were also sampled at 2 kHz.

The pressure response at P1 (the valve) on Figure 8, after the pressure spike, is essentially flat, with only small amplitude, high frequency oscillations. If a reflection of the pressure pulse were to be generated at the elbow, it would arrive at the valve at approximately 20 ms. This is not apparent: the oscillations in this region are a few percent of the initial pressure rise. In the 40-60 ms range larger oscillations occur. These are from the upstream elbows that could not be supported as rigidly.

If there is to be no alteration of the transient, then not only must there be no reflection from the elbow, but no losses at the elbow. Therefore, the pressure at P2 should be the same magnitude as at P1.

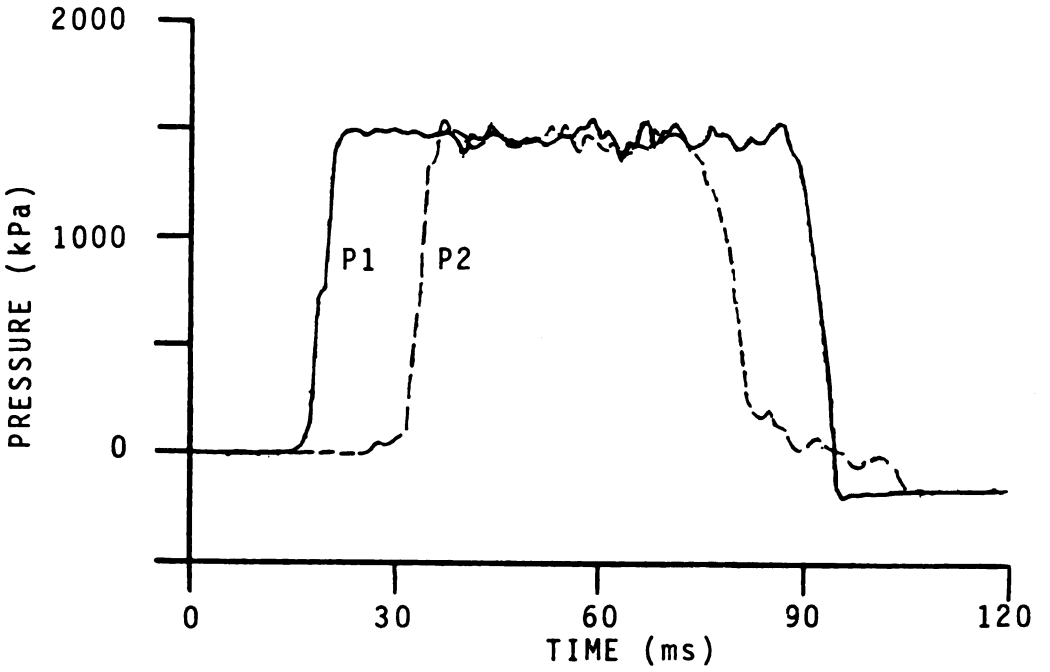

Figure 7. Pressure Response for Case A, Showing Full Pressure Rise

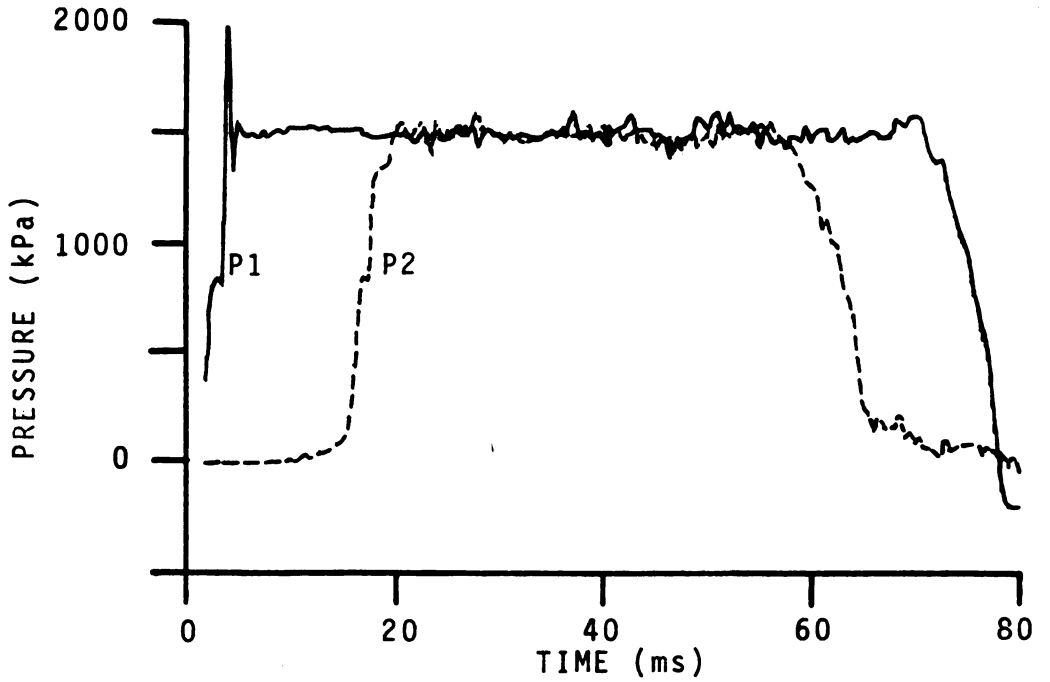

Figure 8. Pressure Response for Case A, Triggered by Pressure Transducer

This is shown to be the case by the dashed line of Figure 8. The average pressures over the pressure surge for P1 and P2 are within 0.3% of each other, showing that the transient is propagated through the elbow with virtually no alteration. If this system were analyzed with a traditional liquid transient model, the predictions would be very similar. The pressure rise predicted by a traditional model is equal to the product of $\rho_f C_f V_0$, which is equal to 1500 kPa in Figure 8.

2.2.3 Case B: Axial Stiffness

As shown on Figure 6, the stiff supports on both sides of elbow 1 are now removed and the elbow is restrained in its plane by the axial stiffness of leg L1 in the x-direction and the axial stiffness of leg L2 in the y-direction. An examination of Figure 9 shows that the pressure response at P1 is significantly different from that of Case A. Elbow motion is initially in the negative x-direction and is driven by the precursor stress wave; this action results in an increase in the liquid pressure. The pressure increase propagates to the valve and is recorded at 13 ms. The elbow motion at 10 ms is the result of the primary pressure pulse driving the elbow in the positive x and y-directions, resulting in a decrease in pressure, as shown on the P1 curve at 20 ms. The elbow then continues to vibrate at the natural frequencies of the fundamental axial modes of reaches L1 and L2 of the piping, and the pressure response

is a combined effect of the resultant velocities.

The maximum pressure, occuring at 44 ms, is 22% above that which would occur in a piping system with no motion ($\rho_f C_f V_0$). The minimum pressure, occuring at 23 ms, is 34% below $\rho_f C_f V_0$. The maximum velocity of the elbow is 0.27 m/s and the maximum displacement is about 0.5 mm.

2.2.4 Case C: Bending Stiffness

For the third case discussed, as shown on Figure 6, the two elbows and the connecting reach L2 are allowed to translate in the y-direction by the flexibility of the attached piping. Because of the relatively large axial stiffness of these short attached lengths, elbow motion in the x-direction is negligible as shown on Figure 10. The effect of the precursor pipe stress on elbow 1 is minimal for this case because of the support. In the y-direction, the frequency of vibration is much lower than that of Case B. The elbow moves first in the positive y-direction when the pressure pulse arrives at the elbow (10 ms). Then as the pulse moves towards elbow 2, there is an elastic return of elbow 1 combined with the pressure pulse arriving at elbow 2 to drive leg L2 in the negative y-direction.

The elbow's motion can again be shown to alter the pressure responses. At P1, after the initial pressure rise, there is a pressure decrease beginning at 20 ms caused by the initial movement of elbow 1 in the positive y-direction.

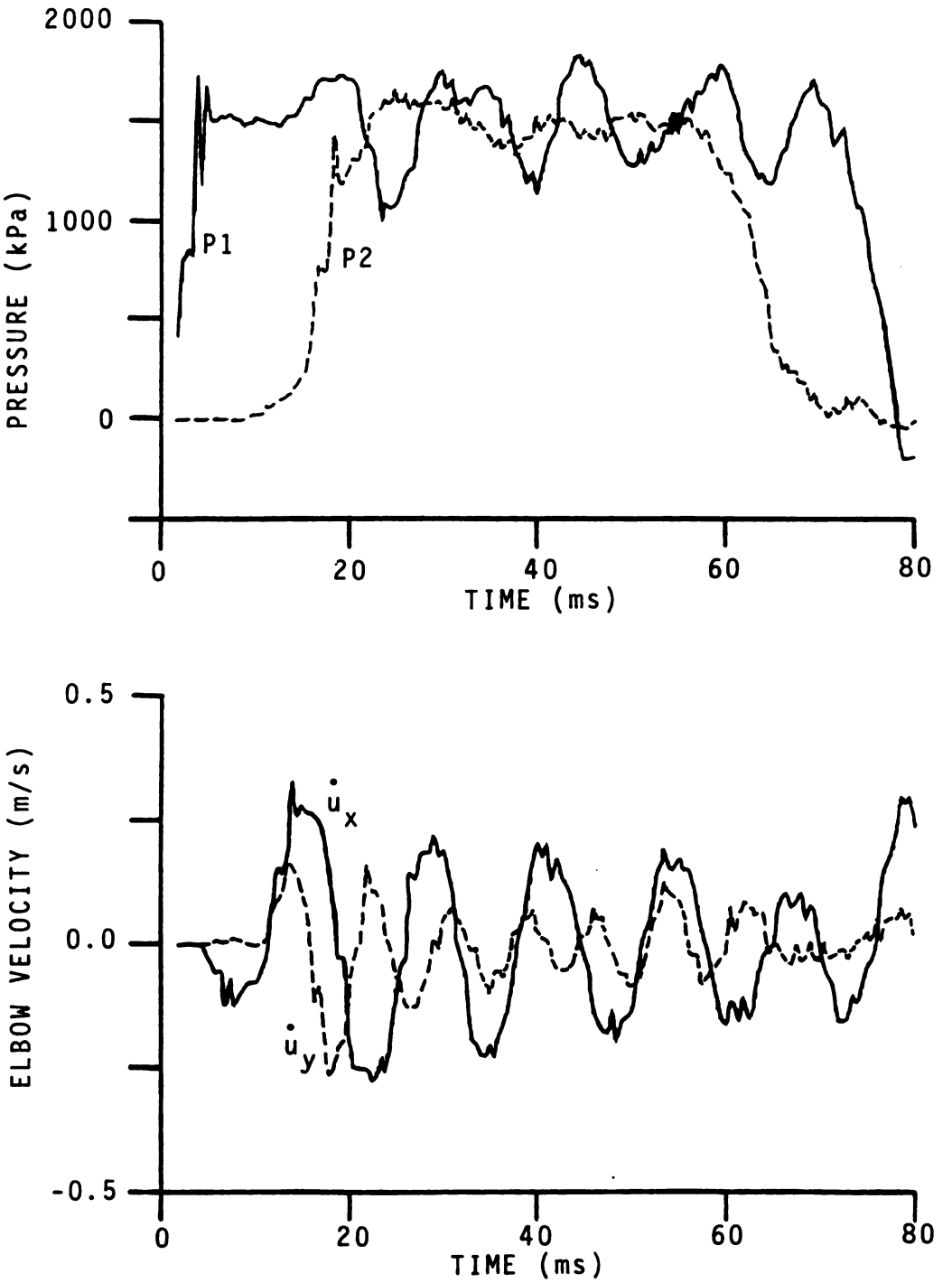

Figure 9. Pressure and Elbow Velocity Responses for Case B

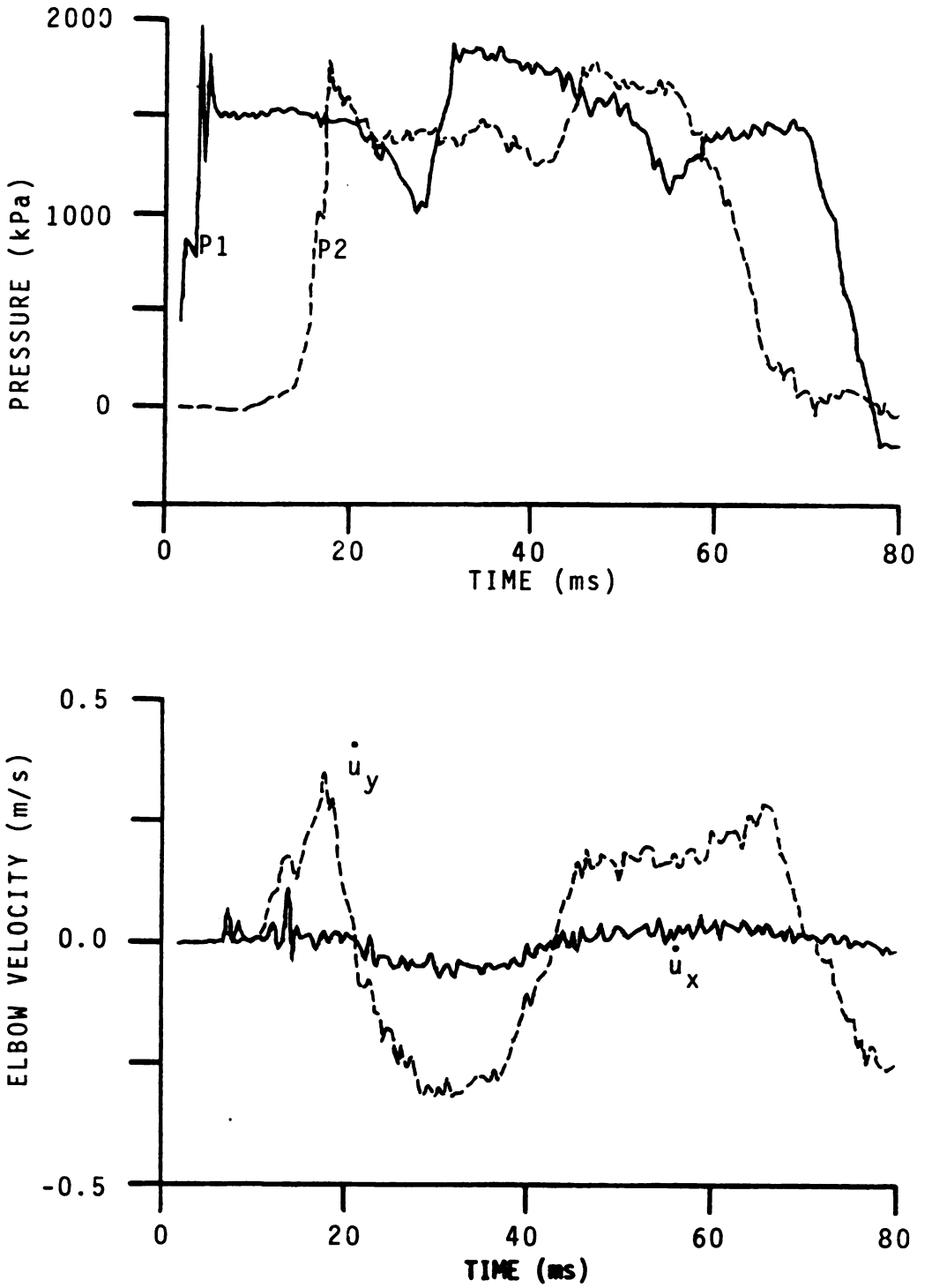

Figure 10. Pressure and Elbow Velocity Responses for Case C

The pressure rise that follows is caused by the combination of two effects: 1) the initial translation of leg L2 in the positive y-direction will cause a pressure increase propagating from elbow 2 back to the valve; and 2) the translation of leg L2 in the negative y-direction will cause a pressure increase propagating from elbow 1 to the valve. The combined effects create a steep pressure increase at P1 at 30 ms. The maximum pressure at P1 is 25% above $\rho_f C_f V_0$ and the minimum is 35% below.

2.2.5 Case D: Combined Effects

As shown on Figure 6, the support near elbow 1 is now removed so that it is restrained by the axial stiffness of leg L1 in the x-direction and the flexural stiffness of one 0.36 m length in the y-direction. For the elbow movement shown in Figure 11, the x-direction velocity is similar to that of Case B, and the y-direction velocity is similar to that of Case C. The resulting pressure shows the high frequency component of Case B superimposed on the low frequency component of Case C. The pressure oscillation is the greatest of all three cases. The maximum pressure at 46 ms is 33% greater than $\rho_f C_f V_0$, and the minimum at 27 ms is 44% below.

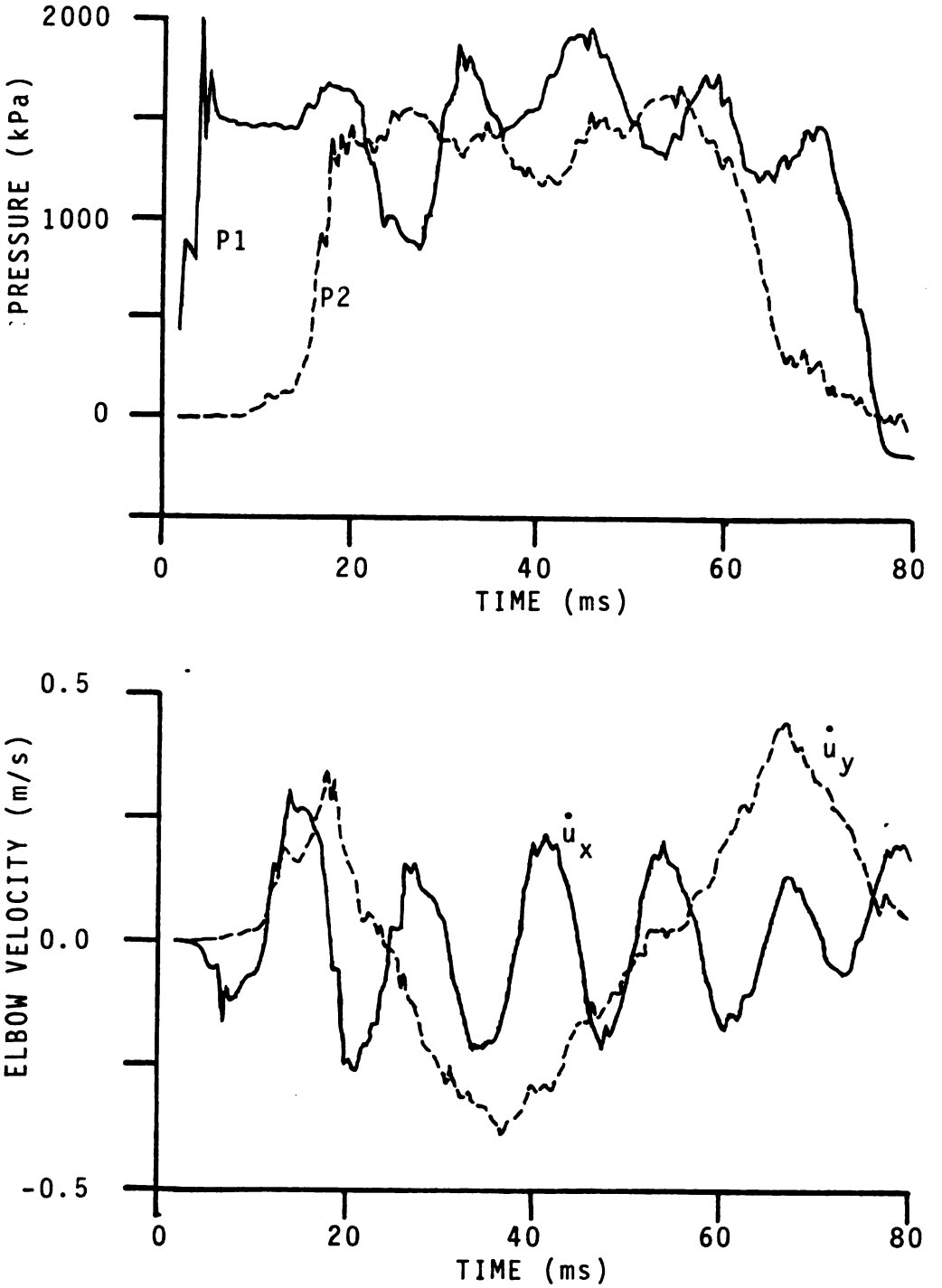

Figure 11. Pressure and Elbow Velocity Responses for Case D

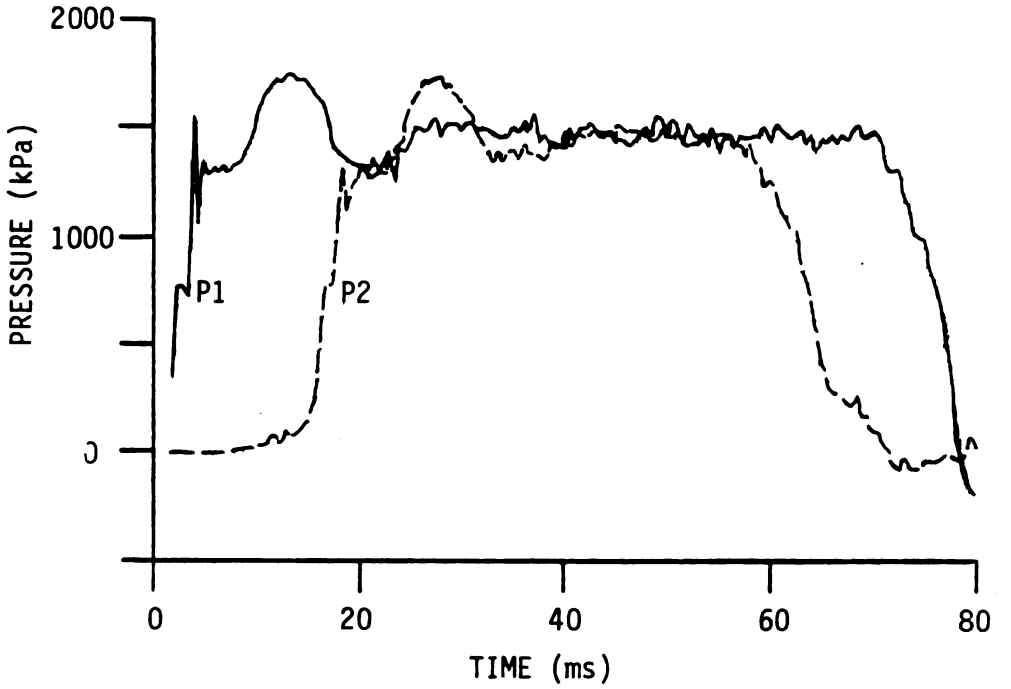

Figure 12. Pressure Response for Case E

2.2.6 Case E: Valve Unrestrained

Figure 12 shows the pressure response due to relaxing the restraint at the valve. The system is set up as in Case A except that the bolts holding down the valve were loosened. The resulting stiffness of the valve in the x-direction is due to the axial stiffness of leg L1 and the restraint provided by attached piping between the valve and pressure tank. This arrangement shows liquid-pipe interaction at a fitting other than an elbow. At P1, the pressure rises initially to a value less than $\rho_f C_f V_0$, due to the valve moving in the negative x-direction. The valve then moves forward and the pressure rises then falls with the oscillations quickly dying out because of damping from the valve and attached piping.

2.2.7 Discussion

Two important observations can be made from the experimental results:

1. If an elbow is fully restrained, there is no observable alteration of a pressure transient travelling through the elbow.

2. If an elbow is not fully restrained, there can be significant alteration of the pressure transient. The alteration is related to the direction and amplitude

of the motion of the elbow, and is, therefore, dependent on the mechanical characteristics of the piping and pipe support structure.

2.2.8 Uncertainty

The pressure transducers and accelerometers were calibrated by the manufacturer, PCB Piezotronics. The manufacturer estimates that the pressure transducers are accurate to within ±3% full scale, resulting in an uncertainty within ±45 kPa. The accelerometers are accurate to within ±3% full scale, resulting in an uncertainty within ±.015 m/s for velocity. These estimates cover the estimated errors between the measurement source and the recording device.

Another possible source of error is the conversion of the analog voltages to digital quantities by the A/D converter. The uncertainty of that process is ±0.03%. The clock is accurate to within ±0.01%.

The copper pipe was manufactured by American Brass Company. They provided tolerances for the inside diameter and wall thickness of the pipe. The inside diameter is manufactured to within ±0.4% or ±0.1 mm and the wall thickness is within ±3% or ±0.04 mm. The measurements of the pipe lengths are accurate to within ±1%.

Chapter 3

THEORY

3.1 Introduction

Internal pressure strains piping circumferentially and axially due to the Poisson effect and due to pressure resultants at fittings such as elbows. The development of a coupled liquid-pipe analysis procedure must include these interactions between the piping and the liquid. A four-equation model is presented that solves for the dependent variables: liquid pressure p, liquid velocity V, axial pipe stress σ_x, and axial pipe velocity $\dot{u}$.

3.2 Four-Equation Model

Walker and Phillips [7] developed a six-equation model that consists of the one-dimensional continuity and momentum equations for the liquid, and the axial and radial momentum equation and two constitutive equations for the pipe wall. The method was developed to study situations where the generation of the transient could be as fast as a few

microseconds. For transients more typical of waterhammer waves generated by valve slam, Walker and Phillips suggested that the inertial term in the radial momentum equation could be neglected and that the classical waterhammer theory was adequate for transient propagation in straight pipes.

The following four-equation model is obtained by neglecting the radial inertia term in Walker and Phillips' model. The main advantage of the simplification is that the time step in the numerical solution can be increased considerably over that of the six-equation model because accurately representing the radial dilation of the pipe wall requires an extremely small time step. The underlying assumptions are one-dimensional flow with uniform p and V over the cross-section, and negligible fluid friction. The pipe is assumed to be linearly elastic, isotropic, prismatic, round and thin-walled. Figure 13 shows the pipe element used for the six-equation model description. The six equations are listed and then simplified to a four-equation system.

Two equations represent the continuity and momentum relations for the liquid:

$$\frac{2}{r}\frac{\partial w}{\partial t} + \frac{1}{K}\frac{\partial p}{\partial t} + \frac{\partial V}{\partial x} = 0 \qquad (2)$$

$$\rho_f \frac{\partial V}{\partial t} + \frac{\partial p}{\partial x} = 0 \qquad (3)$$

The axial and circumferential stress-strain relationships for the pipe wall are:

$$\sigma_x = E^* \left(\frac{\partial u}{\partial x} + \nu \frac{w}{r} \right) \tag{4}$$

$$\sigma_\theta = E^* \left(\frac{w}{r} + \nu \frac{\partial u}{\partial x} \right) \tag{5}$$

where $E^* = E/(1- \nu^2)$ and σ_θ is the circumferential stress. The equations of motion for the pipe in the axial and radial directions are:

$$\frac{\partial \sigma_x}{\partial x} - \rho_t \frac{\partial \dot{u}}{\partial t} = 0 \tag{6}$$

$$\rho_t re \frac{\partial w}{\partial t} = rp - \sigma_\theta e \tag{7}$$

Neglecting the radial momentum term on the left side of equation 7 for waterhammer waves, the circumferential stress can be evaluated for in terms of the pressure:

$$\sigma_\theta = \frac{r}{e} p \tag{8}$$

Combining equations 8 and 5 to eliminate circumferential stress gives:

$$p = \frac{e}{r} E^* \left(\frac{w}{r} + \nu \frac{\partial u}{\partial x} \right) \tag{9}$$

The time derivatives are taken of equations 4 and 9, w is then solved for in equation 9 and substituted into equation 2 and 4, resulting in the two following equations:

$$\left(\frac{1}{K} + \frac{2r}{eE^*}\right)\frac{\partial p}{\partial t} - 2\nu\frac{\partial \dot{u}}{\partial x} + \frac{\partial V}{\partial x} = 0 \qquad (10)$$

$$\frac{\partial \sigma_x}{\partial t} - E\frac{\partial \dot{u}}{\partial x} - \frac{r\nu}{e}\frac{\partial p}{\partial t} = 0 \qquad (11)$$

Equations 3, 6, 10, and 11 are linear, first-order, hyperbolic, partial differential equations describing the behavior of four variables, p, V, σ_x, and $\dot{u}$, which are functions of distance and time. These expressions are an improvement over the classical waterhammer theory since they include dynamic coupling between the liquid and the pipe wall. The coupling exists through the Poisson ratio as seen in equations 10 and 11. The solution of these equations is presented in Chapter 4.

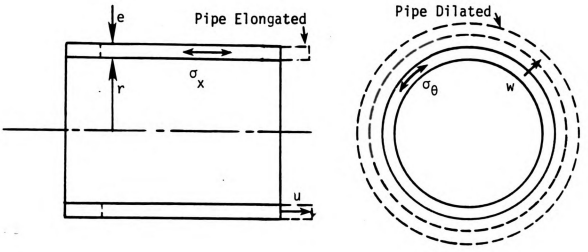

Figure 13. Pipe Element

Chapter 4

NUMERICAL STUDY

4.1 Method of Characteristics

This section describes the solution of the four-equation model presented in the preceding chapter. Equations 3, 6, 10, and 11 are transformed from partial differential equations into ordinary differential equations by the method of characteristics [24]. Characteristic roots are found, and then compatibility relations can be found that are valid along characteristic lines. For the numerical study, the equations are presented in dimensionless form. The parameters are non-dimensionalized as follows:

$$x^* = \frac{x}{r}, \quad t^* = \frac{t a_f}{r}, \quad V^* = \frac{V}{V_0}, \quad p^* = \frac{p}{\rho_f a_f V_0},$$
$$\sigma^* = \frac{\sigma\ 2e}{\rho_f a_f V_0\ r}, \quad \dot{u}^* = \frac{\dot{u}\ 2e}{\rho_f a_f V_0\ r\sqrt{E\rho_t}} \qquad (12)$$

where σ is the axial stress, $a_f = \sqrt{K/\rho_f}$ and the asterisk superscript represents non-dimensional values. For the remaining development the superscript is dropped for

clarity.

Equations 3, 6, 10 and 11 in dimensionless form are:

$$\frac{\partial p}{\partial x} + \frac{\partial V}{\partial t} = 0 \tag{13}$$

$$\frac{\partial \sigma}{\partial x} - W \frac{\partial \dot{u}}{\partial t} = 0 \tag{14}$$

$$J \frac{\partial p}{\partial t} - B \frac{\partial \dot{u}}{\partial x} + \frac{\partial V}{\partial x} = 0 \tag{15}$$

$$\frac{\partial \sigma}{\partial t} - 2\nu \frac{\partial p}{\partial t} - \frac{1}{W} \frac{\partial \dot{u}}{\partial x} = 0 \tag{16}$$

where $$W = \frac{a_f}{a_t} , \quad a_t = (E/\rho_t)^{1/2} \tag{17}$$

$$J = \left(1 + \frac{2rK}{eE} \left(1 - \nu^2 \right) \right)^{1/2} \tag{18}$$

$$B = \frac{\nu r \rho_f}{e \rho_t} W \tag{19}$$

In matrix form, equations 13-16 are:

$$\begin{vmatrix} 0 & 1 & 0 & 0 \\ 0 & 0 & -W & 0 \\ J & 0 & 0 & 0 \\ -2\nu & 0 & 0 & 1 \end{vmatrix} \begin{vmatrix} p \\ V \\ \dot{u} \\ \sigma \end{vmatrix}_t + \begin{vmatrix} 1 & 0 & 0 & 0 \\ 0 & 0 & 0 & 1 \\ 0 & 1 & -B & 0 \\ 0 & 0 & -1/W & 0 \end{vmatrix} \begin{vmatrix} p \\ V \\ \dot{u} \\ \sigma \end{vmatrix}_x = \{ 0 \} \tag{20a}$$

$$[A1] \{ Z \}_t + [A2] \{ Z \}_x = \{ 0 \} \tag{20b}$$

A1 and A2 are coefficient matrices and Z is a column vector containing the dimensionless dependent variables. The

subscripts t and x represent partial differentiation. The characteristic roots (λ) can be obtained by equating the determinate to zero, that is:

$$[\ A2 - \lambda\ A1\ ] = 0 \qquad (21)$$

4.1.1 Wavespeeds

The characteristic roots are the wavespeeds in the liquid-pipe system. The solution of equation 21 yields four roots. The first two roots are the dimensionless liquid wavespeeds, C_f:

$$\lambda_{1,2} = \pm C_f = \pm \frac{1}{J}\, Q1 \qquad (22)$$

and the second two are the dimensionless axial pipe wavespeeds, C_t:

$$\lambda_{3,4} = \pm C_t = \pm \frac{H}{W\ J}\, Q2 \qquad (23)$$

where

$$H = \left(1 + \frac{2rK}{eE} \right)^{1/2} \qquad (24)$$

$$Q1 = \left(1 + \frac{\nu^2\ 2r\rho_f}{e(1-q)\rho_t} \right)^{1/2} \qquad (25)$$

$$Q2 = \left(1 - \frac{\nu^2\ 2r\ \rho_f}{e\ q(1-q)\rho_t} \right)^{1/2} \qquad (26)$$

$$q = H^2 / W^2 \qquad (27)$$

For many piping systems, Q1 and Q2 are close to unity and the wavespeeds can be simplified:

$$C_f = \pm \frac{1}{J} \tag{28}$$

$$C_t = \pm \frac{H}{W\ J} \tag{29}$$

For thin-walled copper pipe filled with water equation 28 differs from equation 22 by less than 2%, and equation 29 differs from equation 23 by less than 1%. Note that equation 28 is the same wavespeed as obtained with traditional analyses considering only the liquid equations and assuming that the pipe is anchored throughout against axial movement; see Wylie and Streeter [2].

4.1.2 Compatibility Equations

In order to eliminate one of the differential operators in equation 20 a linear transformation can be made with a matrix [T] which possesses a non-vanishing determinate:

$$[T]\ [A1]\ \{Z\}_t + [T]\ [A2]\ \{Z\}_x = 0 \tag{30}$$

A useful form of the transformation matrix is:

$$[T]\ [A2] = [\ \lambda\ ]\ [T]\ [A1] \tag{31}$$

where $[\ \lambda\ ]$ is a diagonal matrix composed of the characteristic roots. Let [T] [A1] = [AS] and equation 30 becomes:

$$[AS]\{Z\}_t + [\lambda][AS]\{Z\}_x = 0 \tag{32}$$

which can be written as:

$$[AS]\frac{d}{dt}\{Z\} = 0 \tag{33}$$

valid along the characteristic directions $[\frac{dx}{dt}] = \{\lambda\}$

Solving equation 31 for the transformation matrix [T] and substituting into equation 33 results in the following four dimensionless compatibility equations:

$$\frac{dp}{dt} \pm C_f \frac{dV}{dt} \pm \frac{C_f W}{2\nu}(1-Q1^2)\frac{d\dot{u}}{dt} - \frac{1}{2\nu}(1-Q1^2)\frac{d\sigma}{dt} = 0 \tag{34}$$

valid along $\frac{dx}{dt} = \pm C_f$, and;

$$\frac{dp}{dt} \pm C_t \frac{dV}{dt} \pm \frac{C_t W}{2\nu}(1-qQ2^2)\frac{d\dot{u}}{dt} - \frac{1}{2\nu}(1-qQ2^2)\frac{d\sigma}{dt} = 0 \tag{35}$$

valid along $\frac{dx}{dt} = \pm C_t$

Equations 34 and 35 can be simplified by using the assumptions inherent in equations 28 and 29:

$$\frac{dp}{dt} \pm C_f \frac{dV}{dt} = 0 \tag{36}$$

$$\frac{dp}{dt} \pm C_t \frac{dV}{dt} \pm \frac{H}{2\nu J}(1-q)\frac{d\dot{u}}{dt} - \frac{1}{2\nu}(1-q)\frac{d\sigma}{dt} = 0 \tag{37}$$

Figure 14 shows the characteristic representation in the x-t plane. Equations 34 and 35 are integrated along their respective characteristic lines; the two lines with positive

slope are designated as C+ characteristics, and the two with negative slopes C- characteristics. The following dimensionless finite difference equations result:

$$p_P - p_B + C_f (V_P - V_B) + C_f W G_f (\dot{u}_P - \dot{u}_B) - G_f (\sigma_P - \sigma_B) = 0 \quad (38)$$

$$p_P - p_D - C_f (V_P - V_D) - C_f W G_f (\dot{u}_P - \dot{u}_D) - G_f (\sigma_P - \sigma_D) = 0 \quad (39)$$

$$p_P - p_A + C_t (V_P - V_A) + C_t W G_t (\dot{u}_P - \dot{u}_A) - G_t (\sigma_P - \sigma_A) = 0 \quad (40)$$

$$p_P - p_C - C_t (V_P - V_C) - C_t W G_t (\dot{u}_P - \dot{u}_C) - G_t (\sigma_P - \sigma_C) = 0 \quad (41)$$

$$\text{where } G_f = (1 - Q1^2)/(2\nu), \quad G_t = (1 - q\, Q2^2)/(2\nu) \quad (42)$$

Solution of equations 38-41 consists of dividing the pipeline into elements. The points at the end of the elements are either intermediate locations where information is desired or boundaries that require additional information to solve equations 38-41. For intermediate sections, unknown values at location P are found by simultaneous solution of equations 38-41. For typical piping systems, C_t/C_f is not an integer so timeline interpolations must be made at locations where the characteristic lines fall between time steps. The time step and pipe lengths are chosen so that values for the pipe equations (equations 40 and 41) are not interpolated. Interpolated values are needed for equations 38 and 39, shown as points B and D on Figure 14. At boundaries, only two characteristic lines are available, so two additional relationships must be known to solve for the four unknowns.

4.1.3 Initial Conditions

To begin the solution procedure, initial values of the dependent variables must be established along the pipe. The initial steady-state velocity V_0 is input as data. The initial pressure p_0 is found by calculating the steady-state pressure drop through the valve. Since liquid friction has been neglected, p_0 remains constant throughout the pipe. The initial axial velocity $\dot{u}_0$ is set equal to zero, assuming that the pipe is initially at rest. The initial axial stress σ_0 is caused by the resultant steady-state pressure at the elbows.

4.1.4 Boundary Conditions

The solution of the four-equation system has been described for the intermediate sections of the pipeline. At locations where there are additional constraints imposed on the liquid and/or pipe, boundary conditions must be included in the solution. If the constraint is at the upstream or downstream ends of the piping system, two known conditions must be added to the C- or C+ characteristic equations. If the constraint is not at an end, it is treated as an intermediate section with length equal to zero. Different values of the dependent variables for each side of the section are possible. Following is a description of the reservoir, valve, stiff support, and elbow boundaries.

4.1.4.1 Reservoir

The upstream reservoir adds two known constants to be solved with the C- equations: $p=p_0$, and $\dot{u}=0$ Equations 39 and 41 can then be solved simultaneously for V and σ.

4.1.4.2 Valve

The valve imposes the non-linear relationship between V and p:

$$V = \tau S (p)^{1/2} \qquad (43)$$

where τ is a dimensionless number representing the valve opening: $\tau=1$ for the initial setting, and $\tau=0$ for the valve closed. S is a constant relating the initial flow and pressure. An additional constraint is again $\dot{u}=0$ and equations 38 and 40 are solved simultaneously with equation 43.

4.1.4.3 Stiff Support

The stiff support imposes the following conditions: $p_1=p_2$, $V_1=V_2$, $\dot{u}_1=0$, and $\dot{u}_2=0$; where 1 and 2 are the upstream and downstream sides of the support. Equations 38-41 are then solved simultaneously for the unknowns.

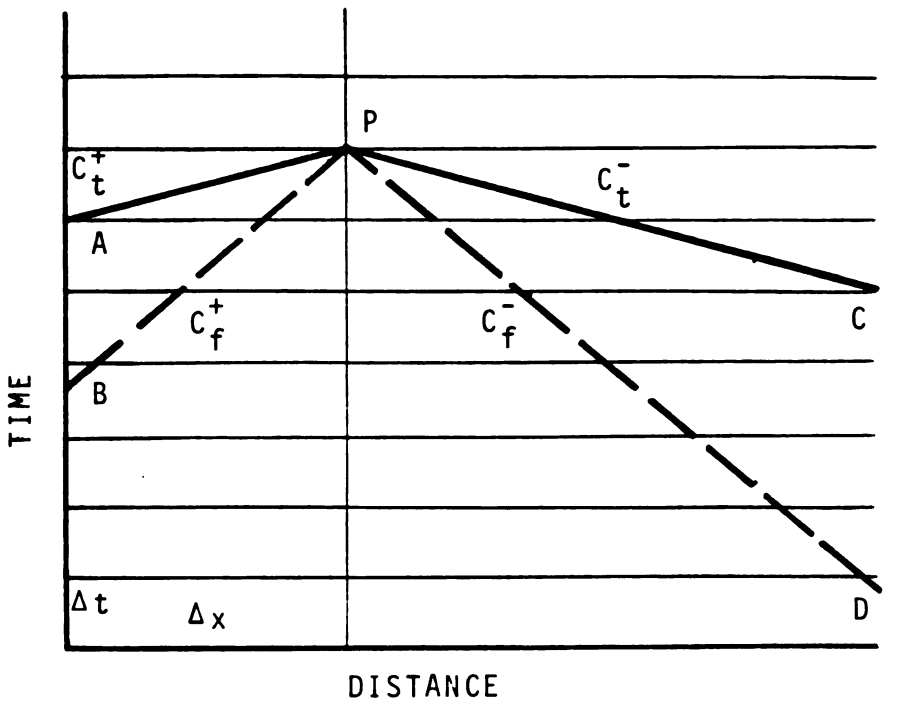

Figure 14. Characteristic Representation

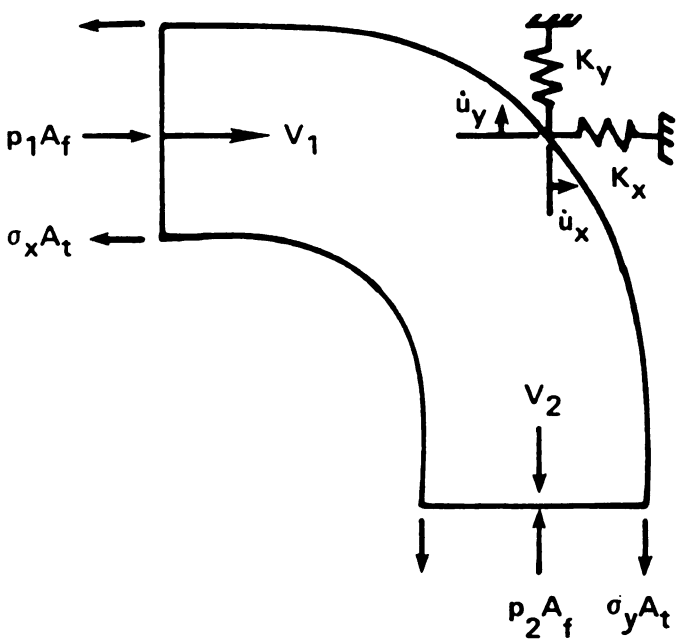

Figure 15. Elbow Schematic

4.1.4.4 Elbow

As presented in Chapter 2, the motion of an elbow alters the behavior of the liquid contained within the pipe. As the elbow moves, it can act to increase or decrease the liquid pressure depending on the direction of motion. The relationship between the liquid and elbow motion is derived from the conservation of mass for a translating control volume. The amount of motion is determined by the equation of motion of the elbow.

The conservation of mass can be written for the control volume shown in Figure 15:

$$\frac{d}{dt} \int_{cv} \rho_f \, d\forall + \int_{cs} \rho_f \vec{V}_r \cdot \hat{n} \, dA = 0 \qquad (44)$$

where V_r is the relative velocity between the liquid and control volume. The elbow is assumed to be rigid and the liquid within it incompressible. Therefore, the time rate of change term can be neglected, resulting in the following relationship:

$$V_{r1} \; A_1 = V_{r2} \; A_2 \qquad (45)$$

For a constant diameter pipe:

$$(V_1 - \dot{u}_x) = (V_2 - \dot{u}_y) \qquad (46)$$

V_1 and V_2 are the upstream and downstream liquid velocities and $\dot{u}_x$ and $\dot{u}_y$ are the elbow velocities in the x and y directions, respectively. Elbow motion is assumed to be planar.

The amplitude of elbow displacement is determined by the equations of motion for the elbow. The four-equation model is solved for the liquid and pipe variables along a straight length of pipe. The axial stiffness of the pipe is included in the equations. To represent the restraint caused by the stiffness of the piping attached perpendicular to the straight length, a simple model is used that lumps stiffness at the elbow, as shown on Figure 15. The equation of motion can be written:

$$p A_f - \sigma A_t = K u \tag{47}$$

where subscripts on cross-sectional area A are f for liquid and t for pipe wall. The lateral liquid momentum force acting on the elbow is neglected in this presentation because of low steady-state flow rates. For situations where the flow rates are a significant percentage of the liquid wavespeed, the lateral momentum force should be included.

The coefficient K is the discrete stiffness used to represent the translation of the attached piping. It is assumed that the attached length of pipe bends in single

curvature (assuming support conditions of one end fixed and the other end free to translate). Any damping attributed to the attached piping is neglected. The mass of the attached piping is neglected for the following reasons: 1) for a short length of pipe, its lateral restraint due to inertia is small compared to its lateral restraint due to stiffness; and 2) for a long length of pipe, the mass can be neglected because during the short duration of observation in this study, the flexural disturbance travels only a short distance; therefore, only a small portion of the pipe length is displaced. For longer duration events, or for intermediate lengths of pipe, the inertia should be included in the analysis.

To solve the elbow boundary, equation 46, equation 47 (imposed in the two orthogonal directions), and equations 38-41 are solved simultaneously with the addition of the following condition: $p_1=p_2$. Equation 47 is integrated by the trapezoidal rule (see Craig [25]) before combining with the other equations.

Note that setting $\dot{u}=0$ at the reservoir, valve, and stiff support implies that the restraint of the pipe at those points is infinitely stiff. It is possible to represent instead the actual structural restraint imposed at that point mathematically, and then solve the resulting system of equations. The representation of the supports mathematically is beyond the scope of this thesis.

The numerical model was developed to determine if the pressures and elbow velocities recorded in the experiment could be predicted with a relatively simple model. Representing the attached piping by a lumped stiffness was possible because the lengths of pipe were extreme, either very long or very short. For a more general piping system, a finite element model of the piping and pipe support structure could be used (see Hatfield, et al. [13]) to provide a more comprehensive model. In the structural analysis, care would need to be taken to avoid including axial modes of the pipe that are already included in the four-equation model.

4.2 Numerical Analysis

The procedures set forth in section 4.1 have been implemented in a computer program called LIQPIP (listing in Appendix). Input data consist of the liquid and pipe properties, valve closure time and loss coefficient, initial flow velocity, and the stiffness coefficients used to represent the attached piping. The configuration of the piping system is input as a series of elements. The three possible element types are a straight length of pipe, an elbow, and a stiff support. The program is able to handle any number of elbows and stiff supports.

4.2.1 Comparison to Experimental Results

The four experimental cases presented in Chapter 4 were simulated with LIQPIP to verify the mathematical model. The steady-state velocity used as input into LIQPIP was calculated from the initial pressure rise from the experimental data. The stiffness coefficients used in the predictions are shown in Table 1. Stiffness coefficients for the translation perpendicular to the long lengths (L1 and L2) are approximated by zero. For the 0.36 m lengths, the coefficients were calculated by the stiffness method (see section 4.2.2.3 for further discussion). The axial stiffness of all the pipe lengths is included in the four-equation model.

Table 1 Stiffness Coefficients

Case	Direction	Elbow	K (N/m)
A	x	1	Infinite
	y	1	Infinite
B	x	1	0
	y	1	0
C	x	1	0
	y	1	94,800
	z	2	0
	y	2	94,800
D	x	1	0
	y	1	0
	z	2	0
	y	2	88,700

4.2.1.1 Case A: Stiff System

Figure 16 shows the predicted pressures at the valve, P1, versus the experimental data. The discrepancies are from the valve flutter at 4 ms and oscillations in the 40-70 ms range as discussed in section 2.2.2. The response predicted by LIQPIP is not flat as would be predicted by a traditional two-equation model, the variation being caused by the second-order Poisson effect.

4.2.1.2 Case B: Axial Stiffness

Figure 17 shows the comparison of pressure, P1, and comparison of elbow 1 velocities for Case B. The phase and the amplitude of the velocity oscillations are predicted accurately. The pressure oscillations resulting from the elbow's movement are predicted slightly higher than the experimental data.

4.2.1.3 Case C: Bending Stiffness

Figure 18 shows a general agreement for the predicted pressure response and for the y-direction elbow velocities. The predicted y-direction elbow velocity is slightly out of phase with the experimental data, suggesting that the estimated stiffness K was too small.

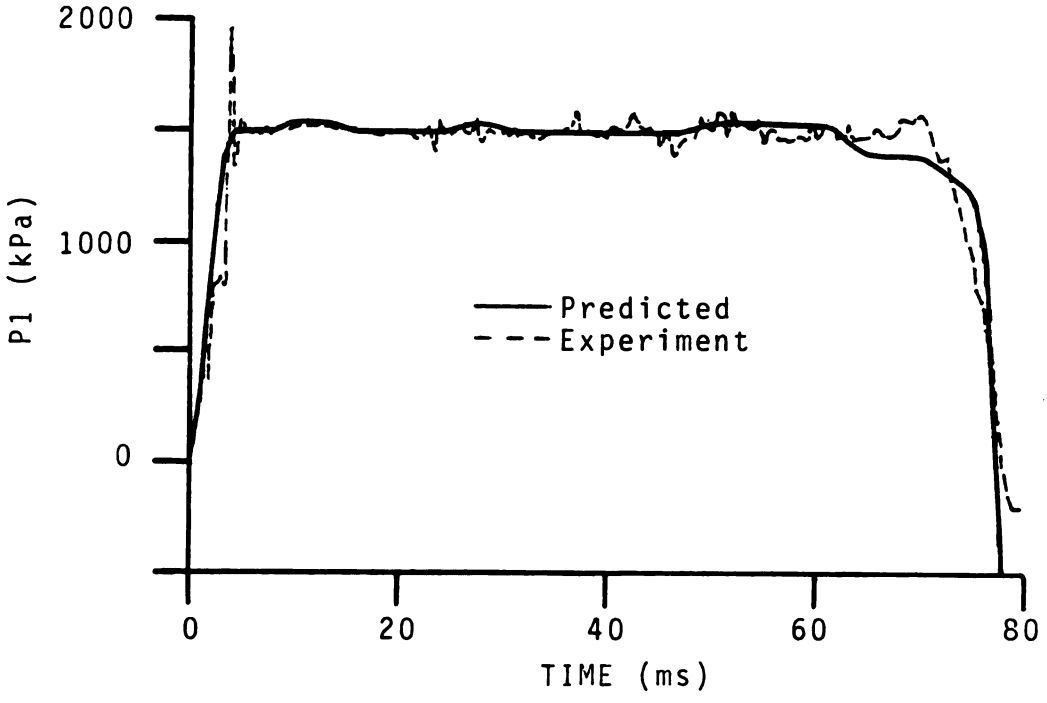

Figure 16. Comparison of Experimental and Predicted Pressures for Case A

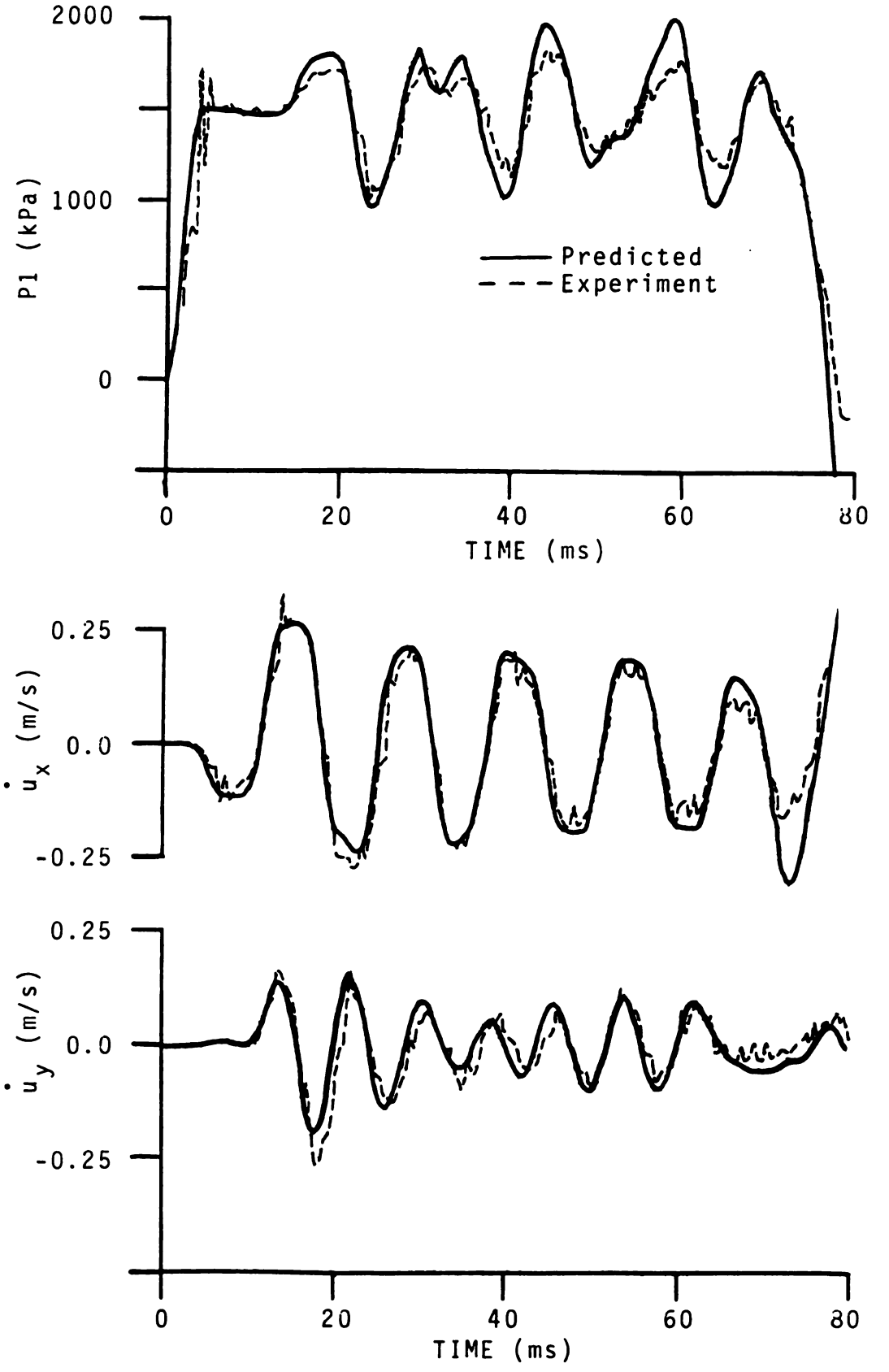

Figure 17. Comparison of Experimental and Predicted Pressures and Elbow Velocities for Case B

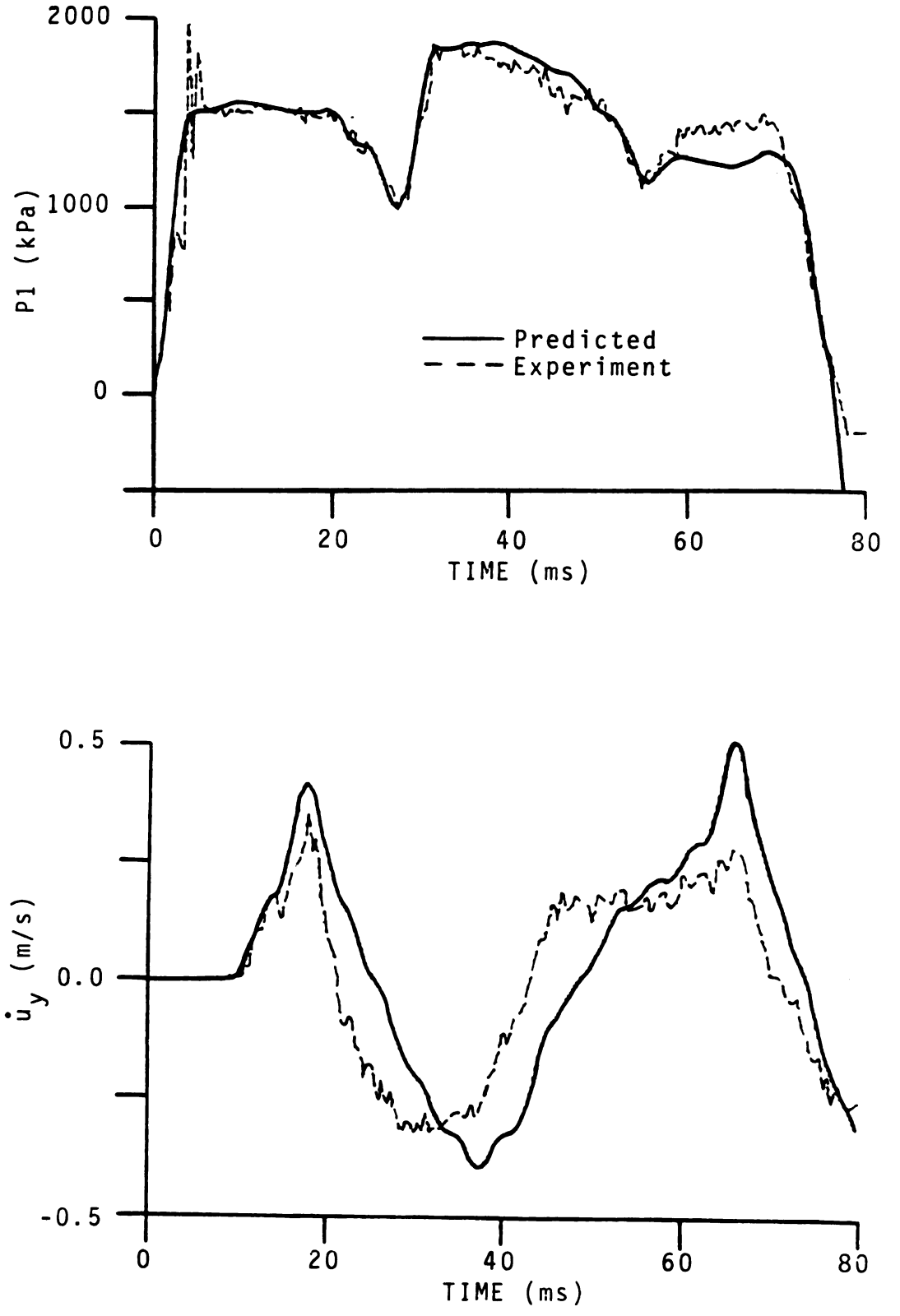

Figure 18. Comparison of Experimental and Predicted Pressures and Elbow Velocities for Case C

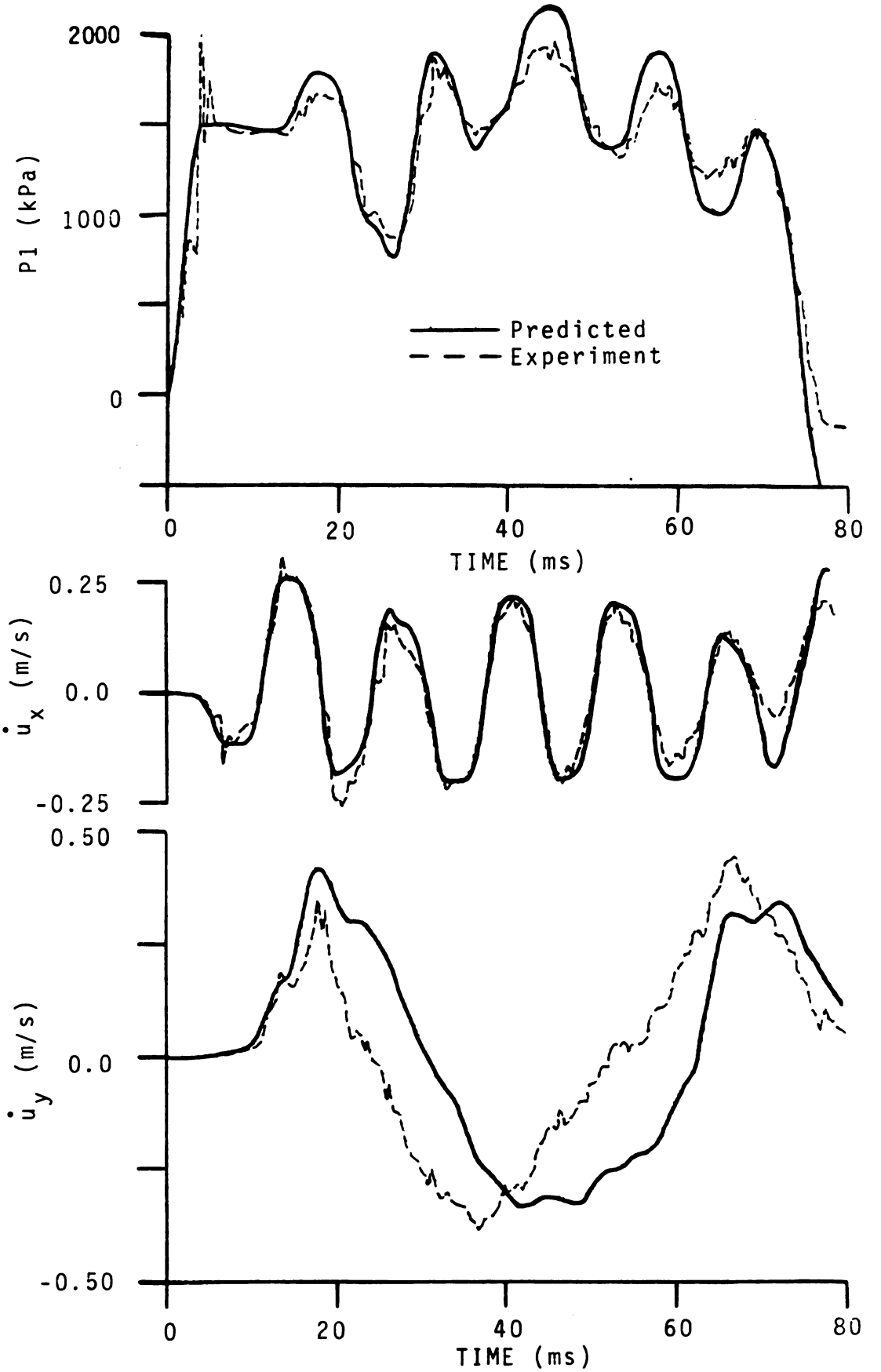

Figure 19. Comparison of Experimental and Predicted Pressures and Elbow Velocities for Case D

4.2.1.4 Case D: Combined

Figure 19 shows small discrepancies in amplitude for the pressure comparison. The x-direction elbow velocity is predicted accurately. The y-direction elbow velocity again is slightly out of phase.

4.2.2 Parametric Study

This section examines some of the important parameters involved in liquid-pipe interaction. The reason for presenting the wavespeeds and compatibility equations in dimensionless form is to reduce the number of parameters needed to describe the behavior of the liquid-pipe system. This section will discuss Poisson ratio effects, the dimensionless parameters that resulted from the equation development, and the stiffness coefficients.

4.2.2.1 Poisson Ratio

The first parameter discussed is Poisson's ratio. As shown in Table 2, the ratio varies from 0.3 for steel to 0.5 for PVC. From the compatibility equations, its importance as a coupling parameter is clearly seen. If Poisson's ratio is set equal to zero, inferring no transformation between axial and circumferential strain, equation 34 becomes uncoupled from equation 35. Equation 34 becomes identically equation 36, and multiplying equation 35 by ν to avoid division by

zero, equation 35 becomes:

$$\pm (1 - q) \frac{d\dot{u}}{dt} - (1 - q) \frac{d\sigma}{dt} = 0 \qquad (48)$$

Equations 36 and 48 are uncoupled equations and are similar to those used by Ellis [19]. Figure 20 shows a comparison of predicted pressures at P1 for Case B, with and without Poisson coupling (Poisson's ratio is set equal to zero for the dashed line). The first pressure rise at 14 ms disappears as would be expected because it is caused by the precursor. With the equations uncoupled, no precursor exists. The magnitude of the resulting oscillations is also reduced.

To gain an understanding of the magnitude of the precursor stress wave, it was desirable to compare the pressure resultant forces and stress forces at an elbow. This is accomplished by comparing the two dynamic forces that drive an elbow as shown in equation 47. A simple system was analyzed with a length of pipe between an elbow and valve. The valve was closed instantaneously and the stress wave (the precursor wave generated by the Poisson effect) and pressure wave were computed. Figure 21 shows the ratio of stress forces in the pipe wall (F_t) to pressure forces in the liquid (F_f) versus r/e.

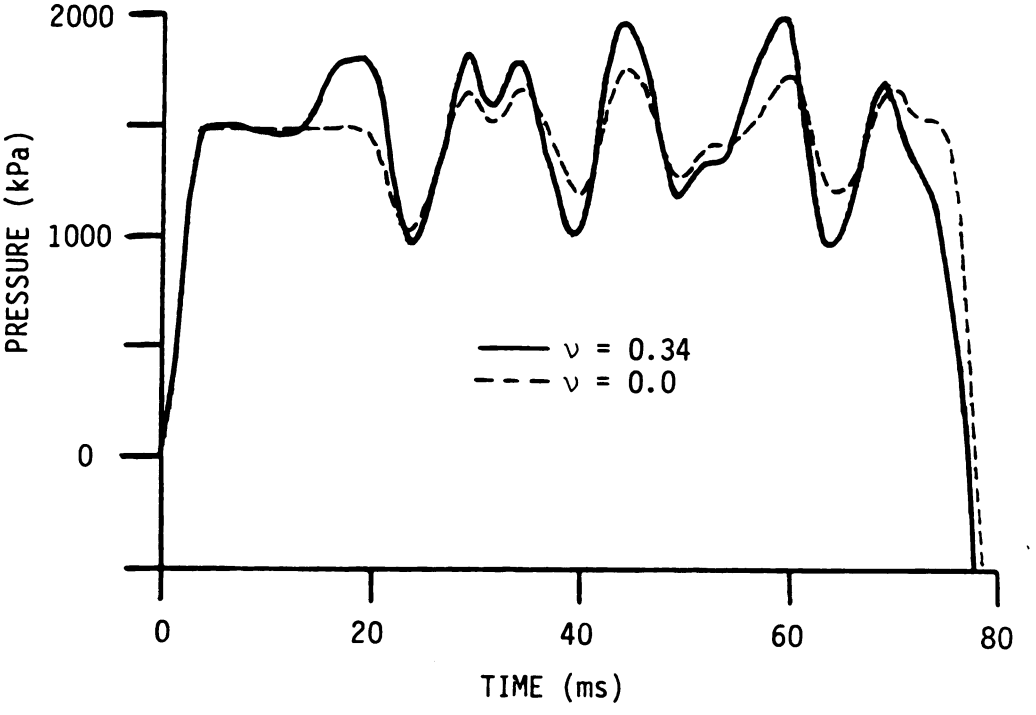

Figure 20. Comparison of Predicted Pressures at P1 for Case B with Variable Poisson Ratio

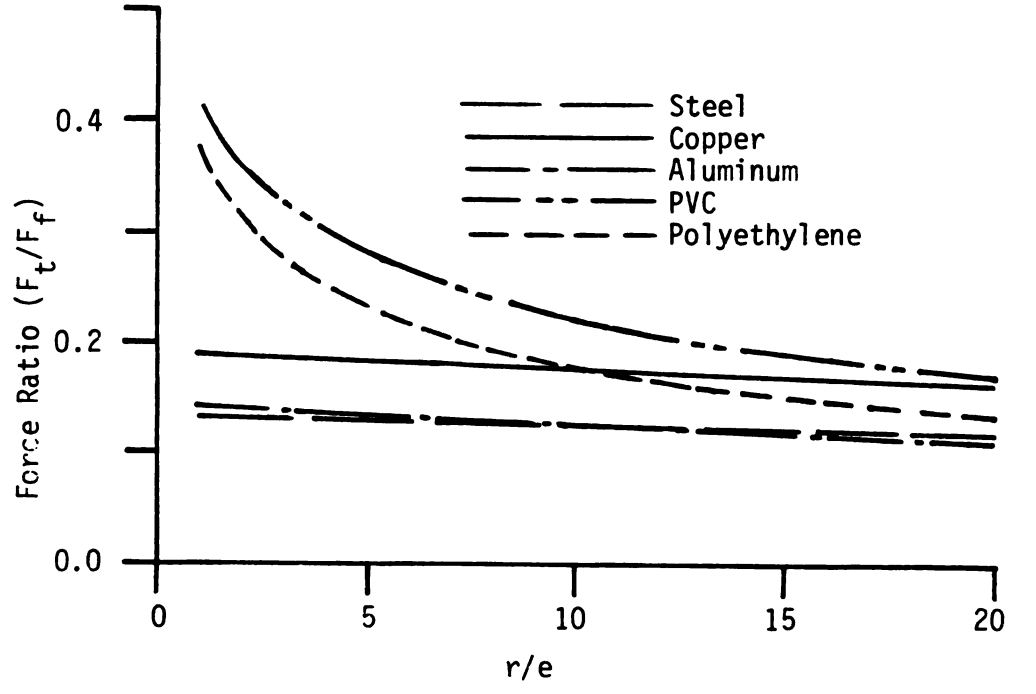

Figure 21. Force Ratio versus r/e

The metal pipes show a stress force equal to 15-20% of the pressure force. In the plastic pipes, the stress force can be as large as 40% of the pressure force for low r/e. The steel, copper, and aluminum pipes show very little dependence on r/e. It should be pointed out that viscoelastic behavior may occur for the polyethylene pipe, a property that has not been included in this study.

4.2.2.2 Dimensionless Parameters

Table 2 lists constants for five different common pipe materials and the dimensionless parameters W, Q1, and Q2. The parameter W, the ratio of liquid and pipe material wavespeeds in an infinite medium, has been calculated using water at 20^{o} C as the contained liquid. The parameter Q1, shown for three r/e ratios, affects mainly the two plastic pipes; it is very close to 1.0 for the metal pipes. The parameter Q2 is very near 1.0 for all cases shown.

Table 2 Pipe Material Constants

Material		Steel	Copper	Aluminum	PVC	Polyethylene
ρ_t(kg/m)		7900	8940	2700	1300	940
ν		0.30	0.34	0.33	0.50	0.46
E (GPa)		211	117	70	2.5	0.86
a_t (m/s)		5160	3620	5090	1390	960
W		0.29	0.41	0.29	1.07	1.55
	r/e					
Q1	5	0.995	0.990	0.986	0.864	0.881
	10	0.992	0.982	0.978	0.865	0.884
	20	0.986	0.973	0.968	0.865	0.886
Q2	5	1.000	1.000	1.001	1.015	1.010
	10	1.001	1.002	1.001	1.008	1.006
	20	1.001	1.003	1.001	1.004	1.003

Figure 22 is a plot of the inverse of the dimensionless parameter J versus r/e for the different pipe materials. This term represents the effect of the circumferential wall stiffness on the liquid wavespeed. From equation 22, assuming Q1=1, for a value of 1/J=1, the dimensionless wavespeed C_f=1. Since the wavespeed is non-dimensionalized by a_f (the wavespeed in an infinite liquid), for 1/J=1, C_f=a_f. As shown in Figure 22, as r/e decreases, 1/J approaches 1 (hence the pipe wall is getting stiffer and its effect on the wavespeed decreases). For aluminum, the wavespeed is reduced by about 30% at r/e=20. For the plastic pipes, the wavespeed is reduced by as much as 90%.

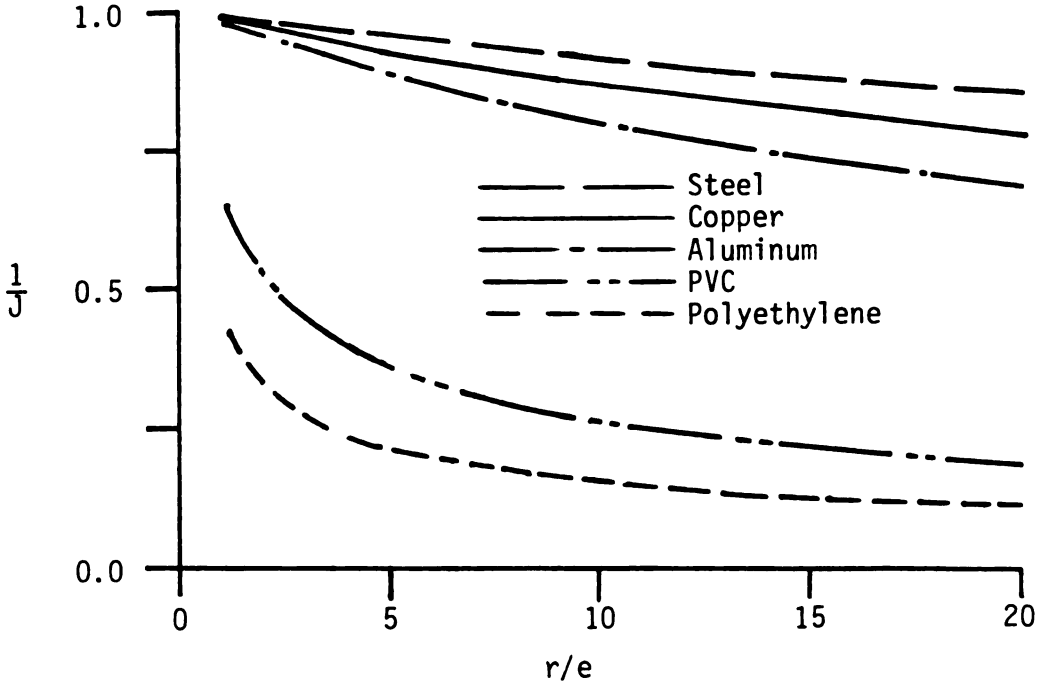

Figure 22. The Inverse of the Dimensionless Parameter J versus r/e

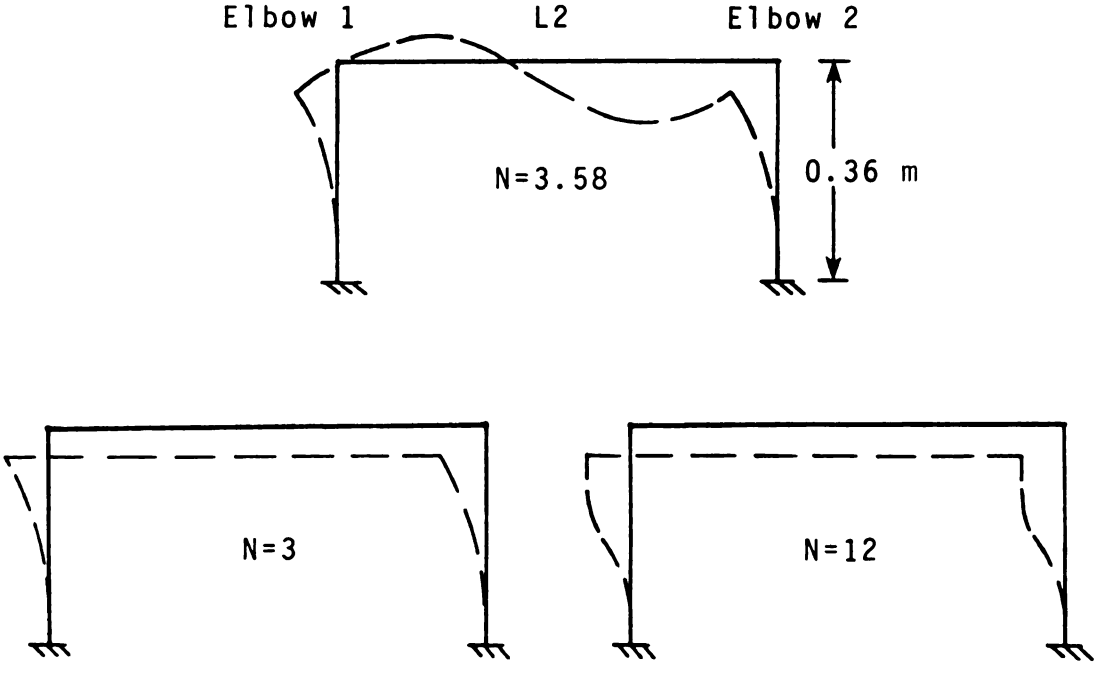

Figure 23. Assumed Deflected Shapes

4.2.2.3 Stiffness Coefficients

The representation of the attached piping at an elbow by a stiffness coefficient was used as a first approximation of the dynamic effects of that portion of the piping system that is not included in the four-equation model. One stiffness coefficient can be input for each elbow axis. In calculating the stiffness coefficient for the short lengths of pipe in Case C and D, the pipe was assumed to be anchored at one end to a stiff support with no rotation possible at that point. The flexural stiffness of the pipe is then calculated as follows:

$$K = N\ EI/L^3 \qquad (49)$$

where E is Young's modulus, I is the moment of inertia of the pipe cross section, and L is the length of the pipe. The constant N ranges from 3 when assuming the elbow end of the pipe to rotate freely (treating the elbow as a hinge), to 12 when assuming no rotation of the pipe at the elbow. The actual rotational fixity is a function of the elbow's geometry and material properties, and the length of attached straight pipes. For Case C and D, the elbows are attached to a long length of pipe (L2=7.6 m). Because of this, the elbows were assumed to be rigid, with any rotation coming from the flexibility of the attached pipes. Case C and D were analyzed by the stiffness method (see White, Gergely,

and Sexsmith [26]). N is equal to 3.58 for Case C and 3.35 for Case D. Figure 23 shows the stuctural configuration and deflected shape used in the calculation of the coefficient for Case C (N=3.58) and for the extreme values of N equal to 3 and 12. Figure 24 shows the effect of N on the predicted pressures and elbow velocities for Case C.

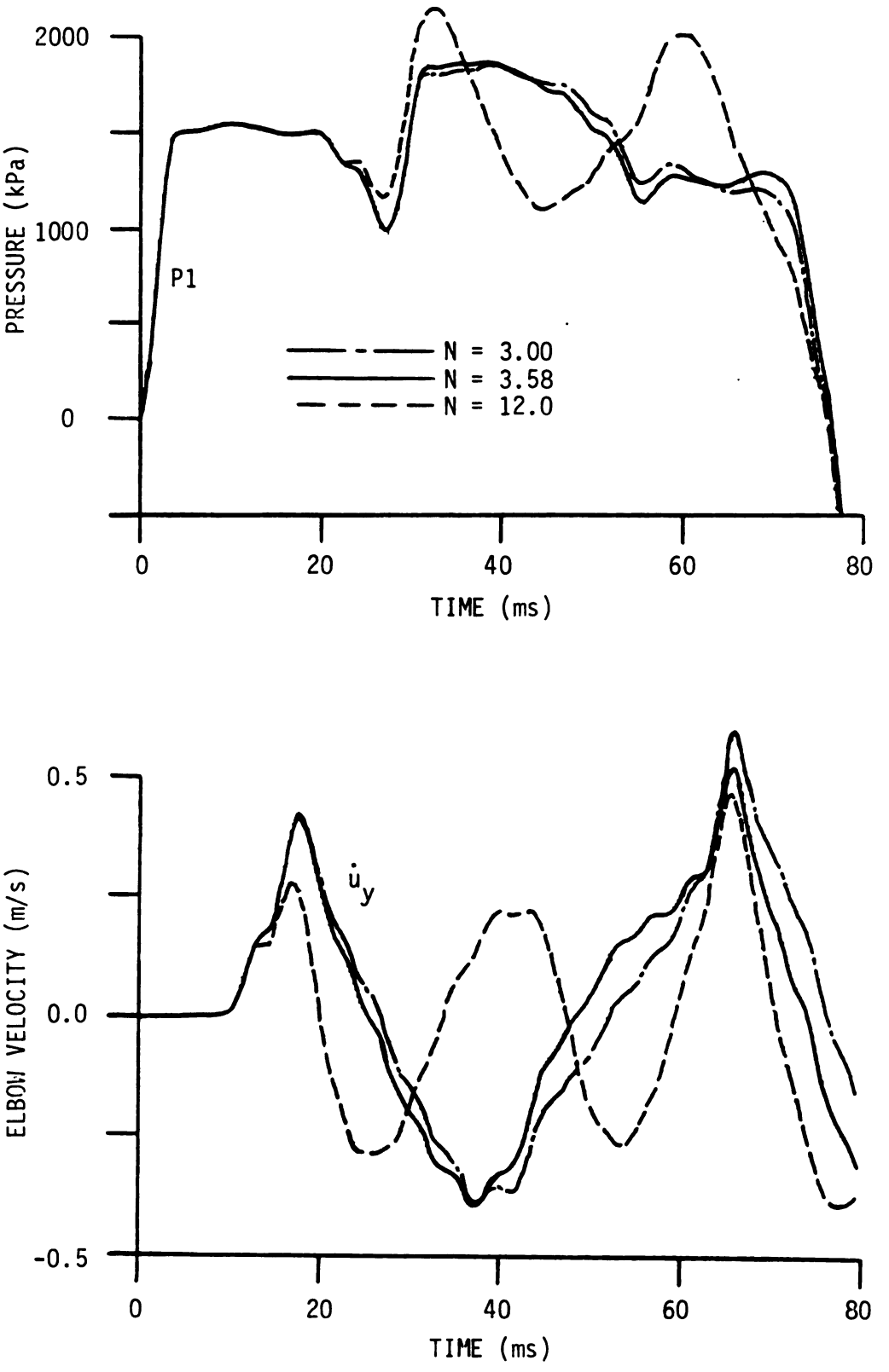

Figure 24. Comparison of Pressures and Elbow Velocities for Case C with Variable Stiffness

Chapter 5

SUMMARY AND CONCLUSIONS

The objective of this thesis was to determine the effect of elbows on a generated pressure transient. It has been demonstrated that the elbow motion is the most important factor in altering the dynamic pressure. The elbow motion is driven by the axial stresses in the pipe and by the liquid pressure. For an elbow that is fully restrained, no significant alteration of the pressure transient occurs. Elbows that are not fully restrained can cause significant alteration of the pressure transient.

An analytical technique was developed that couples liquid and pipe equations to model the interaction. For a straight pipe length, the one-dimensional equations of continuity and momentum for the liquid and pipe wall are solved by the method of characteristics. At an elbow, continuity relationships and an added stiffness component are solved simultaneously with the characteristic equations.

Four experimental configurations were used for verifying the model. The amount of elbow restraint was varied in each setup. In Case A, all the elbows were rigidly supported.

The resulting pressure response was similar to the traditional Joukowsky pressure rise. The predicted pressure response matched the experimental data. In Case B, the supports were removed from the main test elbow. The elbow was then restrained by the axial stiffness of the two connecting pipes. The model predicted the elbow velocities and pressure responses accurately. Elbow motion in Case B was initially due to a precursor wave. The precursor wave is an axial tension wave that is generated by strain-related coupling. The precursor wave travels at approximately the wavespeed in the pipe material. Case C was designed to investigate the translation of a pipe length between two elbows. Stiff supports were located 0.36 m away from each elbow. The pipe between the two elbows could then translate as a function of the structural restraint of the short lengths. The predicted results modeled the general behavior of the elbow velocities and pressure response. The fourth case studied, Case D, combined the axial and translational modes of cases B and C.

In all the cases where the elbow was not restrained, significant alteration of the pressure response occurred. Pressures 33% higher than the traditional Joukowsky pressure rise were recorded.

These results clearly show a need for an increased awareness of the potential for liquid-pipe interaction. The upper limit on the amplification of dynamic pressure by the

elastic response of piping is unknown. In the design of piping systems that are subject to transient pressures and are not supported rigidly, engineers need to consider possible interaction. Rigidity is difficult to achieve, and usually undesirable, in actual pipe hardware and even small flexibility leads to interaction.

Future experimental investigations are needed on more complicated piping configurations with conventional supports. Great care should be taken in documenting the flexibility of the support structure. Damping, which was negligible in the experimental part of this work, could be significant in some systems.

The numerical model predicts the experimental results accurately but needs improvement to be useful for the analysis of a general piping system. Possible improvements could consist of a more complete and general modal representation of the piping structure, material damping coefficients, and damping at discrete supports. The formulation should also be capable of handling a greater variety of hydraulic boundary conditions.

Continuing research into liquid-pipe interaction will lead to improved design of piping by reducing the uncertainties in existing design-analysis procedures.

APPENDIX

A.1 CONTRL Listing

```
C******************CONTRL.FOR*********************************
C               CONTROL PROGRAM FOR MULTICHANNEL A/D SAMPLING
C               WRITTEN BY BOB OTWELL, JUNE 1982
C       MODULES:
C       SAMPL(N(1),NSMPL,NTICK,NRATE,ICHAN,NCHAN,IERR)
C               SAMPLES DATA ON CLOCK INTERUPT AFTER INITIAL TRIGGER
C                       N(1)= SAMPLE BUFFER
C                       NSMPL = NUMBER OF SAMPLES TO TAKE
C                       NTICK = NUMBER OF  TICKS BETWEEN SAMPLES
C                       NRATE = CLOCK RATE (0-7)
C                               0=STOP
C                               1=1 MHZ
C                               2=100 KHZ
C                               3=10 KHZ
C                               4=1 KHZ
C                               5=100 HZ
C                               6=ST1
C                               7=LINE FREQ(60 HZ)
C                       ICHAN = A/D CHANNEL TO SAMPLE (0-15)
C                       NCHAN = NUMBER OF CHANNELS TO SAMPLE
C                       IERR =  NUMBER OF SAMPLING ERRORS
C
C
C
C       LINKING INSTRUCTIONS FOR MODULES:
C       LINK CONTRL,SAMPL
C
C
        LOGICAL*1 FNAME(15)
        DIMENSION V(1000),ACC(250),P(3,250)
        INTEGER N(1000)
        WRITE(7,100)
100     FORMAT(' BEGIN EXECUTION OF CONTRL:',/)
        DO 194 J=1,250
194     ACC(J)=0.
        DO 195 I=1,3
        DO 195 J=1,250
195     P(I,J)=0.
        DO 196 I=1,1000
196     V(I)=0.
C
C       ***************SAMPLING SECTION****************
C
        WRITE(7,105)
105     FORMAT('0ENTER NUMBER OF SAMPLES/CHANNEL: ',$)
        READ(5,110) NSMPL
110     FORMAT(I5)
        WRITE(7,120)
120     FORMAT('0ENTER CLOCK RATE (0-7)',$)
        READ(5,110) NRATE
C   DELT'S ARE IN MS
        IF(NRATE.EQ.1) DELT=.001
        IF(NRATE.EQ.2) DELT=.01
        IF(NRATE.EQ.3) DELT=.1
        IF(NRATE.EQ.4) DELT=1.0
        IF(NRATE.EQ.5) DELT=10.0
        WRITE(7,130)
130     FORMAT('0ENTER NUMBER OF CLOCK TICKS/SAMPLE: ',$)
        READ(5,110) NTICK
```

```
      DELT=DELT*NTICK
      WRITE(7,140)
140   FORMAT('0ENTER FIRST CHANNEL TO SAMPLE: ',$)
      READ(5,110) ICHAN
      WRITE(7,145)
145   FORMAT('0ENTER NUMBER OF CHANNELS TO SAMPLE: ',$)
      READ(5,110) NCHAN
      NSMPT=NSMPL*NCHAN
      IPLOT=0
C
C     ZERO OUT DATA BUFFER;
C
      DO 200 I=1,1000
200   N(I)=0
      WRITE(7,149)
      WRITE(7,150)NRUN,NSMPL,NTICK,NRATE
149   FORMAT(///,' ****************************************',//)
150   FORMAT(1X,'CALLING SAMPLING SUBROUTINE, NRUN =',I5,///,
     1' NSMPL =',I5,//,' NTICK=',I5,//,' NRATE=',I5,/)
      WRITE(7,160) NCHAN,ICHAN
160   FORMAT(' SAMPLING ',I2,' CHANNELS STARTING ON CHANNEL ',I2,/)
C
C     START TO SAMPLE INTO BUFFER 1:
C
      CALL SAMPL(N(1),NSMPL,NTICK,NRATE,ICHAN,NCHAN,IERR)
C
      WRITE(7,170)IERR
170   FORMAT('0**********SAMPLING FINISHED**********',//,
     1I5,' - A/D ERRORS ENCOUNTERED')
220   FORMAT(A1)
      DO 221 I=1,NSMPT
221   V(I)=(N(I)-2048)/400.
C
C     ***************DATA CONVERSION***************
C
C     PUT VOLTAGES INTO ACCELERATION(VELOCITY) AND PRESSURE ARRAYS
C
C
300   WRITE(7,300)
      FORMAT(' DID YOU TAKE ACCELERATION DATA(Y/N)?',$)
      READ(5,220)IACC
      IF(IACC.NE.1HY) GO TO 320
      IPLOT=1
      WRITE(7,305)
305   FORMAT(' WAS IT INTEGRATED(Y/N)?',$)
      READ(5,220)IVEL
C    VOLTAGE TO ACCELERATION(OR VELOCITY) PCB QUARTZ ACCELEROMETERS
C    TRANSDUCERS 5712 AND 5713
C
C   ACCELERATION
      IF(IVEL.NE.1HY)FTSEC2=3214.
C   VELOCITY(FT/SEC)
C     IF(IVEL.EQ.1HY)FTSEC2=1.202
C   VELOCITY(M/SEC)
      IF(IVEL.EQ.1HY)FTSEC2=.3664
      K=0
      DO 310 J=1,NSMPT,NCHAN
      K=K+1
C   ACCELERATION(OR VELOCITY) BUFFER
310   ACC(K)=V(J)*FTSEC2
      NPR1=2
      GO TO 325
320   NPR1=1
325   KK=0
      DO 330 I=NPR1,NCHAN
      K=0
```

```
        KK=KK+1
C    VOLTAGE TO PSI    PCB QUARTZ PRESSURE TRANSDUCERS
C      TRANSDUCER 3808
C    IF(KK.EQ.1)PSI=96.1
C    VOLTAGE TO KPa
        IF(KK.EQ.1)PSI=662.6
C      TRANSDUCER 3809
C      IF(KK.EQ.2)PSI=93.3
        IF(KK.EQ.2)PSI=643.2
C      TRANSDUCER 3810
C      IF(KK.EQ.3)PSI=98.4
        IF(KK.EQ.3)PSI=678.4
        DO 330 J=I,NSMPT,NCHAN
        K=K+1
330     P(KK,K)=V(J)*PSI
C
C       PRINT SAMPLE DATA
C
        WRITE(7,265)
265     FORMAT('ODO YOU WANT TO SEE VALUES(Y/N)?',$)
        READ(5,220)IPRR
        IF(IPRR.NE.1HY) GO TO 229
        IF(IACC.NE.1HY) GO TO 420
        WRITE(7,410)(ACC(I),I=1,NSMPL)
410     FORMAT(8F9.2)
420     KK=0
        DO 430 J=NPR1,NCHAN
        KK=KK+1
430     WRITE(7,410)(P(KK,I),I=1,NSMPL)
C
C
C**********VELOCITY PLOTS***************
C
229     IF(IVEL.NE.1HY) GO TO 894
        WRITE(7,810)
810     FORMAT('ODO YOU WANT A VELOCITY PLOT(Y/N)?',$)
        READ(5,220)IVL
        IF(IVL.NE.1HY) GO TO 895
        CALL GTLIN(FNAME,'ENTER UDOT FILENAME')
        OPEN(UNIT=1,NAME=FNAME,TYPE='NEW')
        WRITE(1,820)
820     FORMAT(';UDOT FILE')
        T=0.0
        DO 870 I=1,NSMPL
        WRITE(1,860) T,ACC(I)
860     FORMAT('RD',2G15.7)
870     T=T+DELT
        WRITE(1,880)
880     FORMAT('ED')
        CLOSE(UNIT=1)
        GO TO 895
C
C*********ACCELERATION PLOTS***********
C
894     WRITE(7,910)
910     FORMAT('ODO YOU WANT AN ACCELERATION PLOT(Y/N)?',$)
        READ(5,220)IAC
        IF(IAC.NE.1HY) GO TO 895
        CALL GTLIN(FNAME,'ENTER ACC FILENAME')
        OPEN(UNIT=1,NAME=FNAME,TYPE='NEW')
        WRITE(1,920)
920     FORMAT(';ACC FILE')
        T=0.0
        DO 970 I=1,NSMPL
        WRITE(1,960) T,ACC(I)
960     FORMAT('RD',2G15.7)
```

```
970     T=T+DELT
        WRITE(1,980)
980     FORMAT('ED')
        CLOSE(UNIT=1)
C
C
C       ***************PRESSURE PLOTS***************
C
895     WRITE(7,510)
510     FORMAT('ODO YOU WANT PRESSURE PLOTS(Y/N)?',$)
        READ(5,220)IPR
        IF(IPR.NE.1HY) GO TO 999
        CALL GTLIN(FNAME,'ENTER P1 FILENAME')
        OPEN(UNIT=1,NAME=FNAME,TYPE='NEW')
        WRITE(1,9)
  9     FORMAT(';P1 FILE')
        NPR2=NCHAN-IPLOT
        IF(NPR2.EQ.1) GO TO 16
        CALL GTLIN(FNAME,'ENTER P2 FILENAME')
        OPEN(UNIT=2,NAME=FNAME,TYPE='NEW')
        WRITE(2,8)
  8     FORMAT(';P2 FILE')
        IF(NPR2.EQ.2) GO TO 16
        CALL GTLIN(FNAME,'ENTER P3 FILENAME')
        OPEN(UNIT=3,NAME=FNAME,TYPE='NEW')
        WRITE(3,11)
 11     FORMAT(';P3 FILE')
 16     DO 501 J=1,NPR2
        T=0.0
        DO 39 I=1,NSMPL
        WRITE(J,29) T,P(J,I)
 29     FORMAT('RD',2G15.7)
 39     T=T+DELT
        WRITE(J,49)
 49     FORMAT('ED')
501     CONTINUE
        CLOSE(UNIT=1)
        IF(NPR2.GT.1)CLOSE(UNIT=2)
        IF(NPR2.GT.2)CLOSE(UNIT=3)
999     CONTINUE
        CALL EXIT
        END
```

A.2 SAMPL Listing

```
        .TITLE SAMPL.MAC
        ;WRITTEN BY BOB OTWELL JUNE 1982
        ;SAMPL IS AN INTERUPT-DRIVEN, CLOCKED SAMPLING
        ;SUBROUTINE.  SAMPLING BEGINS WITH A POSITIVE VOLTAGE
        ;CROSSING OF THE SCHMITT TRIGGER 2 LEVEL AND CONTINUES
        ;FOR A SPECIFIED TIME
        ;
        ;CALLED FROM FORTRAN MAIN PROGRAM WITH:
        ;   CALL SAMPLE(IBUF(1),NSAMPL,NTICK,NRATE,ICHAN,NCHAN,ERROR)
        ;        IBUF=SAMPLE ARRAY
        ;        NSMPL=NUMBER OF SAMPLES
        ;        NTICK=NUMBER OF CLOCK TICKS/SAMPLE
        ;        NRATE=CLOCK TICK RATE
        ;        ICHAN=FIRST CHANNEL NUMBER
        ;        NCHAN=NUMBER OF CHANNELS TO BE SAMPLED
        ;        ERROR=NUMBER OF ERRORS WHILE SAMPLING
        ;
        .GLOBL SAMPL
COUNT:  0
ERROR:  0
TEMPCK: 0
TEMPAD: 0
NCHAN:  0
COCHAN: 0
DFLG:   0
ADDR:   .WORD 0
        ADVEC1=400
        ADVEC2=402
        ERVEC1=404
        ERVEC2=406
        ADSR=177000
        ADSR1=177001
        ADBR=177002
        CLKSR=170420
        CLKBR=170422
        TTPDB=177566
SAMPL:
        CLR ERROR               ;INITIALLIZING THE A/D ERROR COUNT TO 0
        CLR DFLG                ;INITIALLIZING THE DONE FLAG
        MOV 2(R5),ADDR          ;BEGINNING ADDRESS OF SAMPLE OUTPUT BUFFER
        MOV @4(R5),R0           ;NUMBER OF SAMPLES
        MOV @6(R5),R1           ;T=# OF CLOCK TICKS
        NEG R1                  ;
        MOV R1,@#CLKBR          ;PUT -T INTO CLOCK BUFFER
        MOV @10(R5),TEMPCK      ;CLOCK RATE
        ASL TEMPCK              ;SET UP CLOCK RATE
        ASL TEMPCK              ; BITS 3-5
        ASL TEMPCK              ;
        BIC #177707,TEMPCK      ;ZERO OTHER BITS
        BIS #20002,TEMPCK       ;CLOCK STATUS:
                                ;REPEATED INTERVAL
                                ;START WHEN SCHMIDT TRIGGER 2 FIRES
        MOV @12(R5),TEMPAD      ;GET FIRST CHANNEL NUMBER
        BIC #177600,TEMPAD      ;ZERO OTHER BITS
        SWAB TEMPAD             ;SWAP BYTES
        BIS #040140,TEMPAD      ;SET UP A/D STATUS:
                                ;ENABLE REAL TIME CLOCK
                                ;INTERRUPT WHEN A/D IS DONE
```

```
                                    ;INTERRUPT FOR AN A/D CONVERSION ERROR
        MOV #ISR1,@#ADVEC1          ;SET UP BEEP ISR VECTOR
        MOV #340,@#ADVEC2           ;PRIORITY 7
        MOV #ERR,@#ERVEC1           ;SET UP A/D ERROR ISR VECTOR
        MOV #340,@#ERVEC2           ;PRIORITY 7
        MOV @14(R5),NCHAN           ;GET NUMBER OF CHANNELS TO SAMPLE
        MOV NCHAN,COCHAN            ;SET UP CHANNEL COUNTER
        MOV TEMPAD,@#ADSR           ;LOADING A/D STATUS REGISTER
        MOV R0,COUNT                ;MAXIMUM NUMBER OF SAMPLES
        MOV TEMPCK,@#CLKSR          ;LOADING CLOCK STATUS REGISTER

AGAIN.  WAIT                        ;WAITING FOR AN INTERRUPT
        TST DFLG                    ;ARE WE FINISHED ?
        BEQ AGAIN                   ;BACK FOR MORE WAITING
        RTS PC                      ;RETURN TO THE MAIN PROGRAM
                                    ;
ISR1:   MOV #007,@#TTPDB            ;BEEP WHEN SAMPLING BEGINS
        MOV #ISR2,@#ADVEC1          ;SET UP A/D DONE ISR VECTOR
                                    ;
ISR2:                               ;A/D DONE SERVICE ROUTINE
SERV21: MOV @#ADBR,@ADDR            ;MOVE A/D SAMPLE TO THE BUFFER
        ADD #2,ADDR                 ;POINT TO THE NEXT BUFFER ADDRESS
        DEC COCHAN
        BEQ SERV29                  ;ALL CHANNELS SAMPLED
        INCB @#ADSR1                ;NO, INCREMENT CHANNEL
        BIS #1,@#ADSR               ;START NEXT SAMPLE
SERV22: TSTB @#ADSR                 ;SAMPLE DONE?
        BMI SERV21                  ;YES, GO GET IT
        JMP SERV22                  ;NO WAIT SOME MORE
SERV29: DEC COUNT.                  ;DECREMENT SAMPLE COUNT
        BEQ STOP                    ;ENOUGH SAMPLES TAKEN ?
        MOV TEMPAD,@#ADSR           ;NO, SET UP A/D AGAIN
        MOV NCHAN,COCHAN            ;RESET CHANNEL COUNTER
        RTI                         ;RETURN FOR MORE A/D SAMPLES ON CLKOV
                                    ;
                                    ;
ERR.                                ;A/D ERROR SERVICE ROUTINE
        INC ERROR                   ;COUNTING THE NUMBER OF A/D ERRORS
        BIC #100200,ADSR            ;CLEAR ERROR CONDITION
        BIC #200,@#CLKSR            ;CLEAR THE OVERFLOW FLAG
        RTI                         ;
                                    ;
STOP:   CLR @#CLKSR                 ;STOP THE CLOCK
        MOV ERROR,@16(R5)           ;PASSING THE NUMBER OF ERRORS TO FORTRAN
        MOV #1,DFLG                 ;SIGNAL THAT ALL SAMPLES ARE TAKEN
        RTI                         ;CLEANING UP REMAINING INTERRUPT
        .END SAMPL
```

A.3 LIQPIP Listing

```
C
C*****************LIQPIP ---LIQUID-PIPE/SDOF*************************
C               WRITTEN BY BOB OTWELL, SPRING 1983
C               LAST UPDATE NOV. 1983
C     LIQPIPS IS A COUPLED FLUID/PIPE ANALYSIS PROGRAM
C     1. A FOUR EQUATION MODEL CONSISTING OF THE ONE DIMENSIONAL EQUATIONS
C        OF CONTINUITY AND MOMENTUM FOR THE FLUID AND PIPE WALL ARE SOLVED
C        BY THE METHOD OF CHARACTERISTICS(MOC)
C     2. STRUCTURAL RESTRAINT CAUSED BY PIPE SUPPORTS AND ATTACHED PIPING
C        IS REPRESENTED AS TWO SDOF SPRING/MASS/DASHPOT SYSTEMS AT EACH ELBOW
C        THE ELBOW BOUNDARY CONSISTS OF SOLVING 7-EQUATIONS(4 MOC, 1 CONTINUITY,
C        AND 2 SDOF EQUATIONS OF MOTION) SIMULTANEOUSLY. THE EQUATIONS OF
C        MOTION ARE INTEGRATED BY THE AVERAGE ACCELERATION METHOD AS OUTLINED
C        IN "STRUCTURAL DYNAMICS" BY CRAIG (PG 148)
C     3. ANOTHER INTERMEDIATE BOUNDARY CONSISTS OF A STIFF SUPPORT WHERE
C        UDOT IS SET EQUAL TO ZERO
C     4. THE UPSTREAM BOUNDARY IS A CONSTANT HEAD RESERVOIR
C     5. THE DOWNSTREAM BOUNDARY IS A VALVE
C
C
C   THE PROGRAM IS SUBDIVEDED INTO THE FOLLOWING SECTIONS
C
C               1. MAIN PROGRAM -CONTROL OF TIME AND SUBROUTINES
C               2. READP        -INPUT PIPE AND FLUID DATA
C               3. READS        -INPUT SDOF DATA
C               4. PIPE         -SOLUTION OF 4-EQUATION MODEL
C               5. PRINT        -PRINTING SUBROUTINE
C               6. PLOT         -PLOTTING SUBROUTINE
C
C       THE MAIN VARIABLES ARE:
C            INDEPENDENT
C               X       -DISTANCE ALONG PIPE AXIS
C               T       -TIME
C            DEPENDENT
C               P(X,T)  -FLUID PRESSURE
C               V(X,T)  -FLUID AXIAL VELOCITY
C               SGX(X,T)-PIPE AXIAL STRESS
C               UDT(X,T)-PIPE AXIAL VELOCITY
C
C       CONSTANTS
C
C               CF      -FLUID WAVESPEED
C               CT      -PIPE WAVESPEED
C               DT      -TIME STEP
C               TC      -VALVE CLOSURE TIME
C               VO      -INITIAL FLOW VELOCITY
C               PRES    -INITIAL PRESSURE
C               R       -INSIDE RADIUS OF PIPE
C               ET      -WALL THICKNESS
C               K       -FLUID BULK MODULUS
C               E       -MODULUS OF ELASTICITY
C               KNU     -POISSON'S RATIO
C               RHOF    -FLUID DENSITY
C               RHOT    -PIPE DENSITY
C               SK      -SDOF STIFFNESS
C               SM      -SDOF MASS
C               SC      -SDOF DAMPING
C
       COMMON/PASS/JJ,T,SK(4),SM(4),SC(4)
```

```
      COMMON/P/P(15,50),V(15,50),SQX(15,50),UDT(15,50),
      1XL(15),NTYP(15)
      COMMON/CONST/PI,XLMIN,PRES,S,TMAX,TC,DT,KOUNT,KPLOT,NSTDY,
      1ND,NELM,NELBW,IP1,IP2,IP3,IU1,IU2,J1,J2,J3,J4,J5,PJOUK
      COMMON/PLOT/TPLT(200),UPLT(2,200),PPLT(3,200),KK
      LOGICAL*1 FNAME(15)
C
      CALL GTLIN(FNAME,' ENTER PRINT FILE NAME ')
      OPEN(UNIT=1,NAME=FNAME,TYPE='NEW')
      WRITE(1,10)FNAME
10    FORMAT(4X,'FILENAME IS ',A15)
      CALL READP
      IF(NELBW.NE.0)CALL READS
C
C   STEADY-STATE SETUP
C
C   T  -TIME
C   JJ -COUNTER FOR MOC
C   JJC-COUNTER FOR KOUNT AND KPLOT
C   KK -COUNTER FOR PLOTTING
C
      T=0.
      JJ=1
      JJC=1
      KK=1
      CALL PIPE
      CALL PRINT
      WRITE(7,1)
1     FORMAT(4X,'DO YOU WISH TO CONTINUE WITH TRANSIENT
      1SOLUTION(Y/N)?',$)
      READ(5,2)IRUN
2     FORMAT(A1)
      IF(IRUN.NE.1HY) GO TO 99
C
C   TRANSIENT SOLUTION
30    T=T+DT
      IF(T.GT.TMAX) GO TO 99
      JJ=JJ+1
      JJC=JJC+1
      CALL PIPE
      IF(JJC/KOUNT*KOUNT.EQ.JJC)CALL PRINT
      IF(KPLOT.EQ.0) GO TO 30
      IF(JJC/KPLOT*KPLOT.NE.JJC) GO TO 30
      KK=KK+1
      TPLT(KK)=T*1000.
C   SUBTRACT PRES SO DYNAMIC PRESSURE IS PLOTTED
      PPLT(1,KK)=(P(IP1,JJ)-PRES)*S
      PPLT(2,KK)=(P(IP2,JJ)-PRES)*S
      PPLT(3,KK)=(P(IP3,JJ)-PRES)*S
C   MULT UDOT1 BY -1 TO MODEL ACCELEROMETERS
      UPLT(1,KK)=-UDT(IU1,JJ)
      UPLT(2,KK)=UDT(IU2,JJ)
      GO TO 30
99    CONTINUE
      CLOSE(UNIT=1)
      IF(KPLOT.NE.0)CALL PLOT
      CALL EXIT
      END
C*************************************************************************
      SUBROUTINE READP
      COMMON/P/P(15,50),V(15,50),SQX(15,50),UDT(15,50),
      1XL(15),NTYP(15)
      COMMON/CONST/PI,XLMIN,PRES,S,TMAX,TC,DT,KOUNT,KPLOT,NSTDY,
      1ND,NELM,NELBW,IP1,IP2,IP3,IU1,IU2,J1,J2,J3,J4,J5,PJOUK
      WRITE(7,1)
      WRITE(1,1)
```

```
1       FORMAT(/,4X,'***TIME DATA***',/,4X,'INPUT TMAX(MS),TC(MS),
        1NSTDY')
        READ(5,*)TMAX,TC,NSTDY
        WRITE(1,10)TMAX,TC,NSTDY
10      FORMAT(6X,F8.2,F10.2,I5)
        WRITE(7,2)
        WRITE(1,16)
2       FORMAT(/,4X,'***PIPE DATA***',/,4X,'INPUT NUMBER OF
        1ELEMENTS ',$)
16      FORMAT(/,4X,'***PIPE DATA***')
        READ(5,*)NELM
        WRITE(7,3)
        WRITE(1,17)
3       FORMAT(/,4X,'INPUT ELEMENT TYPE, LENGTH(M)')
17      FORMAT(21X,'TYPE      LENGTH')
        XLTOT=0.
        XLMIN=1000.
        DO 5 I=1,NELM
        WRITE(7,4)I
4       FORMAT(4X,'ELEMENT',I3,2X,$)
        READ(5,*)NTYP(I),XL(I)
        XLTOT=XL(I)+XLTOT
        IF(XL(I).LT.XLMIN.AND.XL(I).NE.0)XLMIN=XL(I)
5       CONTINUE
        DO 20 I=1,NELM
        WRITE(1,12)I,NTYP(I),XL(I)
12      FORMAT(4X,'ELEMENT',I3,5X,I5,F10.3)
20      CONTINUE
        NRCH=0
        NELBW=0
        NSTIFF=0
        DO 6 I=1,NELM
        IF(NTYP(I).EQ.1)NRCH=NRCH+1
        IF(NTYP(I).EQ.2)NELBW=NELBW+1
6       IF(NTYP(I).EQ.3)NSTIFF=NSTIFF+1
        WRITE(7,7)NRCH,NELBW,NSTIFF,XLTOT
        WRITE(1,7)NRCH,NELBW,NSTIFF,XLTOT
7       FORMAT(/,4X,'THERE ARE',I3,' PIPE REACHES',I3,' ELBOWS,
        1 AND',I3,' STIFF SUPPORTS',/,4X,' THE TOTAL PIPE LENGTH
        1 IS',F7.3,/)
        WRITE(7,8)
8       FORMAT(4X,'INPUT JOUKOVSKY PRESSURE RISE(KPA) ',$)
        READ(5,*)PJOUK
        RETURN
        END
C*****************************************************************************
        SUBROUTINE READS
        COMMON/PASS/JJ,T,SK(4),SM(4),SC(4)
        COMMON/CONST/PI,XLMIN,PRES,S,TMAX,TC,DT,KOUNT,KPLOT,NSTDY,
        1ND,NELM,NELBW,IP1,IP2,IP3,IU1,IU2,J1,J2,J3,J4,J5,PJOUK
        ND=2*NELBW
        WRITE(7,1)ND
1       FORMAT(4X,'***SDOF DATA***',//,4X,'INPUT FOR',I3,'  SDOFS')
        WRITE(7,2)
        WRITE(1,6)
2       FORMAT(5X,'INPUT STIFFNESS, MASS, AND
        1 DAMPING FACTOR',/)
6       FORMAT(15X,'STIFFNESS    MASS       DAMPING',/)
        DO 4 I=1,ND
        WRITE(7,3)I
3       FORMAT(4X,'DOF ',I3,2X,$)
        READ(5,*)SK(I),SM(I),SC(I)
        WRITE(1,5)I,SK(I),SM(I),SC(I)
5       FORMAT(4X,'DOF ',I3,2X,3F10.3)
        IF(SK(I).EQ.0)SK(I)=1.E-9
        IF(SM(I).EQ.0)SM(I)=1.E-9
```

```
      IF(SC(I).EQ.0)SC(I)=1.E-9
4     CONTINUE
      RETURN
      END
C*************************************************************************
      SUBROUTINE PIPE
      COMMON/PASS/JJ,T,SK(4),SM(4),SC(4)
      COMMON/P/P(15,50),V(15,50),SQX(15,50),UDT(15,50),
     1XL(15),NTYP(15)
      COMMON/CONST/PI,XLMIN,PRES,S,TMAX,TC,DT,KOUNT,KPLOT,NSTDY,
     1ND,NELM,NELBW,IP1,IP2,IP3,IU1,IU2,J1,J2,J3,J4,J5,PJOUK
      COMMON/PLOT/TPLT(200),UPLT(2,200),PPLT(3,200),KK
      DIMENSION JALQT(15),JALQF(15),THETA(15),SKST(4),SKM(4),E1(2)
     1,E2(2),E3(2),E4(2),EB(2),DE(2),U0(4),U1D(4),U2D(4)
      REAL K,KNU
C     DATA STATEMENT IS USED FOR PIPE AND FLUID DATA
C     FLUID--WATER@25C,  PIPE--1" TYPE L COPPER
      DATA R,ET,K,E,KNU,RHOF,RHOT/.013,.00127,2.2E9,1.17E11
     1,.0034,998.2,8900./
C
      IF(T.GT.0)GO TO 30
C
      NSFT=25
      NSFT2=2*NSFT
      JJMX=0
      ESTR=E/(1.-KNU*KNU)
      TAU=1.
      CDA0=.0001
      PI=3.1416
      RM=R+ET/2
      Z1=RHOT/(2.*RHOF)
      Z2=E/(2.*K)+RM/ET
      Z3=2.*RHOT*RM/ET
      CF=SQRT((-Z2-Z1+SQRT((Z2-Z1)**2+Z3*KNU**2/RHOF))/
     1(Z3/E*(KNU**2-1.)-RHOT/K))
      CT=SQRT((-Z2-Z1-SQRT((Z2-Z1)**2+Z3*KNU**2/RHOF))/
     1(Z3/E*(KNU**2-1.)-RHOT/K))
      TMAX=TMAX/1000.
      TC=TC/1000.
      S=1./1000.
      DT=XLMIN/CT
      DT2=DT*DT
      NPTS=NELM+1
      NELM1=NELM-1
      TSTDY=NSTDY*DT
      TC=TC+TSTDY
      XMULT=CT/CF
      DO 9 I=1,NELM
      JALQT(I)=XL(I)/XLMIN
      ALQF=XMULT*JALQT(I)
      JALQF(I)=ALQF
      IF(JALQF(I).GT.JJMX)JJMX=JALQF(I)
      THETA(I)=ALQF-JALQF(I)
      WRITE(7,17)XL(I),XLMIN,THETA(I),JALQT(I),ALQF,JALQF(I)
17    FORMAT(4X,3F6.3,I5,F7.2,I5)
9     CONTINUE
      AF=PI*R*R
      AP=PI*((R+ET)**2-R*R)
      QA=(RHOF*CF*CF*(2.*RM/ESTR+ET/K)-ET)/(KNU*R)
      QC=(RHOF*CT*CT*(2.*RM/ESTR+ET/K)-ET)/(KNU*R)
      QCA=QC/QA
      B1=RHOF*CF
      C1=RHOT*CF*QA
      B2=RHOF*CT
      C2=RHOT*CT*QC
      BC=(B2-C2)/(B1-C1)
```

```
      QCA1=1.-QC/QA
      QM=QC-QA
      B21=B2/B1
      Z5=(B2-QC*B1/QA)/(AF*QCA1)
C     CONSTANTS FOR ELBOW BOUNDARY
      IF(NELBW.EQ.0) GO TO 12
      D1=1.+QA*AF/AP
      D2=1.+QC*AF/AP
      DO 10 I=1,ND
      SKST(I)=SK(I)+2.*SC(I)/DT+4.*SM(I)/DT2
10    SKM(I)=1.-SK(I)/SKST(I)-SM(I)*4./(DT2*SKST(I))
      DO 11 I=1,NELBW
      I1=2*I-1
      I2=2*I
      E1(I)=B1-QA*SC(I1)/(AP*SKM(I1))-C1
      E2(I)=B2-QC*SC(I1)/(AP*SKM(I1))-C2
      E3(I)=QA*SC(I2)/(AP*SKM(I2))+C1-B1
      E4(I)=QC*SC(I2)/(AP*SKM(I2))+C2-B2
      EB(I)=B2*E1(I)-B1*E2(I)
11    DE(I)=D2*E1(I)-D1*E2(I)
      WRITE(7,15)R,ET,K,E,RHOF,RHOT,KNU
15    FORMAT(/,4X,'R,ET,K,E= ',2F8.5,2E10.3,/,
      14X,'RHOF,RHOT,KNU= ',2F7.1,F6.3)
      WRITE(1,15)R,ET,K,E,RHOF,RHOT,KNU
C
C
C*****STEADY-STATE SETUP*****
C
12    PJOUK=PJOUK/S
      VO=PJOUK/(RHOF*CF)
      PRES=RHOF*(AF*VO/CDAO)**2/2.
      WRITE(7,13)VO,CF,CT,PRES*S,PJOUK*S
13    FORMAT(/,4X,'VO= ',F6.3,'M/S,   CF,CT= ',2F7.1,'M/S',/,
      14X,'PRES,PJOUK= ',F6.3,F7.1,'KPA')
      WRITE(1,13)VO,CF,CT,PRES*S,PJOUK*S
      CVP=VO*VO*AF*AF/(2.*PRES)
      SGXO=PRES*AF/AP
      FORC10=PRES*AF-SGXO*AP
      FORC20=-FORC10
C
C     INITIALIZE ARRAYS
C
      DO 20 I=1,NPTS
      V(I,1)=VO
      P(I,1)=PRES
      SGX(I,1)=SGXO
20    UDT(I,1)=0.
      DO 25 I=1,ND
      UO(I)=0.
      U10(I)=0.
25    U20(I)=0.
      TPLT(1)=0.
      UPLT(1,1)=0.
      UPLT(2,1)=0.
      PPLT(1,1)=0.
      PPLT(2,1)=0.
      PPLT(3,1)=0.
      RETURN
C
C*****TRANSIENT SOLUTION*****
30    CONTINUE
      IF(NELBW.EQ.0) GO TO 41
C
C     ELBOW BOUNDARY
C
C     J IS COUNTER FOR ELBOW
```

```
C    JS1 IS COUNTER FOR FIRST SDOF
C    JS2 IS COUNTER FOR SECOND SDOF
C    I1 IS COUNTER FOR UPSTREAM POINT
C    I2 IS COUNTER FOR DOWNSTREAM POINT
          JS1=-1
          J=0
          DO 40 I=2,NELM1
          IF(NTYP(I).NE.2) GO TO 40
          J=J+1
          JS1=JS1+2
          JS2=JS1+1
          I1=I
          I2=I+1
          JT1=JJ-JALQT(I-1)
          IF(JT1.LT.1)JT1=1
          JT2=JJ-JALQT(I+1)
          IF(JT2.LT.1)JT2=1
          JF1=JJ-JALQF(I-1)
          IF(JF1.LT.1)JF1=1
          JF2=JJ-JALQF(I+1)
          IF(JF2.LT.1)JF2=1
          JF11=JF1-1
          IF(JF11.LT.1)JF11=1
          JF21=JF2-1
          IF(JF21.LT.1)JF21=1
          THET1=THETA(I-1)
          THET2=THETA(I+1)
          T11=1.-THET1
          T12=1.-THET2
C
          PR=T11*P(I-1,JF1)+THET1*P(I-1,JF11)
          VR=T11*V(I-1,JF1)+THET1*V(I-1,JF11)
          SQXR=T11*SQX(I-1,JF1)+THET1*SQX(I-1,JF11)
          UDTR=T11*UDT(I-1,JF1)+THET1*UDT(I-1,JF11)
          PS=T12*P(I2+1,JF2)+THET2*P(I2+1,JF21)
          VS=T12*V(I2+1,JF2)+THET2*V(I2+1,JF21)
          SQXS=T12*SQX(I2+1,JF2)+THET2*SQX(I2+1,JF21)
          UDTS=T12*UDT(I2+1,JF2)+THET2*UDT(I2+1,JF21)
          CP1=PR+B1*VR-C1*UDTR+QA*SQXR
          CP2=P(I-1,JT1)+B2*V(I-1,JT1)-C2*UDT(I-1,JT1)+QC*SQX(I-1,JT1)
          CM1=PS-B1*VS+C1*UDTS+QA*SQXS
          CM2=P(I2+1,JT2)-B2*V(I2+1,JT2)+C2*UDT(I2+1,JT2)+QC*SQX(I2+1,JT2)
C
          FORC1=P(I1,JJ-1)*AF-SQX(I1,JJ-1)*AP-FORC10
          FORC2=-P(I2,JJ-1)*AF+SQX(I2,JJ-1)*AP-FORC20
          CN1=(4.*SM(JS1)/DT+2.*SC(JS1))*U10(JS1)+2.*SM(JS1)*U20(JS1)
          CN2=(4.*SM(JS2)/DT+2.*SC(JS2))*U10(JS2)+2.*SM(JS2)*U20(JS2)
          CT1=-U20(JS1)+4.*(-U0(JS1)-U10(JS1)*DT)/DT2
          CT2=-U20(JS2)+4.*(-U0(JS2)-U10(JS2)*DT)/DT2
          CF1=U0(JS1)+(CN1-FORC1)/SKST(JS1)
          CF2=U0(JS2)+(CN2-FORC2)/SKST(JS2)
          SKC1=SK(JS1)*CF1+SM(JS1)*(CT1+4.*CF1/DT2)+FORC10
          SKC2=SK(JS2)*CF2+SM(JS2)*(CT2+4.*CF2/DT2)+FORC20
          F1=CP1+QA*SKC1/(AP*SKM(JS1))
          F2=CP2+QC*SKC1/(AP*SKM(JS1))
          EF=E2(J)*F1-F2*E1(J)
          F3=-CM1+QA*SKC2/(AP*SKM(JS2))
          F4=-CM2+QC*SKC2/(AP*SKM(JS2))
C
          P(I1,JJ)=(E4(J)*(B1*EF+EB(J)*F3)-(B2*EF+EB(J)*F4)*E3(J))/
          1((EB(J)*D2+B2*DE(J))*E3(J)-E4(J)*(EB(J)*D1+B1*DE(J)))
          P(I2,JJ)=P(I1,JJ)
          UDT(I2,JJ)=-(P(I1,JJ)*(D1+B1*DE(J)/EB(J))+EF*B1/EB(J)+F3)/E3(J)
          V(I2,JJ)=UDT(I2,JJ)-(P(I1,JJ)*DE(J)+EF)/EB(J)
          UDT(I1,JJ)=(-P(I1,JJ)*D1-V(I2,JJ)*B1+UDT(I2,JJ)*B1+F1)/E1(J)
          V(I1,JJ)=V(I2,JJ)+UDT(I1,JJ)-UDT(I2,JJ)
```

```
      SGX(I1,JJ)=P(I1,JJ)*AF/AP-(SKC1+SC(JS1)*UDT(I1,JJ))/(AP*SKM(JS1))
      SGX(I2,JJ)=P(I1,JJ)*AF/AP+(SKC2+SC(JS2)*UDT(I2,JJ))/(AP*SKM(JS2))
      U1D(JS1)=UDT(I1,JJ)
      U1D(JS2)=UDT(I2,JJ)
      UD(JS1)=CF1+(P(I1,JJ)*AF-SGX(I1,JJ)*AP-FORC1D)/SKST(JS1)
      UD(JS2)=CF2+(-P(I2,JJ)*AF+SGX(I2,JJ)*AP-FORC2D)/SKST(JS2)
      U2D(JS1)=CT1+4.*UD(JS1)/DT2
      U2D(JS2)=CT2+4.*UD(JS2)/DT2
40    CONTINUE
C
C   UPSTREAM RESERVOIR
C
41    UDT(1,JJ)=0.
      P(1,JJ)=PRES
      JT2=JJ-JALGT(1)
      IF(JT2.LT.1)JT2=1
      JF2=JJ-JALGF(1)
      IF(JF2.LT.1)JF2=1
      JF21=JF2-1
      IF(JF21.LT.1)JF21=1
      THET2=THETA(1)
      T12=1.-THET2
      PS=T12*P(2,JF2)+THET2*P(2,JF21)
      VS=T12*V(2,JF2)+THET2*V(2,JF21)
      SGXS=T12*SGX(2,JF2)+THET2*SGX(2,JF21)
      UDTS=T12*UDT(2,JF2)+THET2*UDT(2,JF21)
      CM1=PS-B1*VS+C1*UDTS+GA*SGXS
      CM2=P(2,JT2)-B2*V(2,JT2)+C2*UDT(2,JT2)+GC*SGX(2,JT2)
      SGX(1,JJ)=(P(1,JJ)*(1.-B21)-CM2+B21*CM1)/(B21*GA-GC)
      V(1,JJ)=(P(1,JJ)-CM1+GA*SGX(1,JJ))/B1
C
C   STIFF SUPPORT
C
      DO 50 I=2,NELM
      IF(NTYP(I).EQ.3)GO TO 45
      IF(NTYP(I).EQ.2)GO TO 50
      IF(NTYP(I-1).EQ.1)GO TO 47
      GO TO 50
45    I1=I
      I2=I+1
      JT1=JJ-JALGT(I-1)
      IF(JT1.LT.1)JT1=1
      JT2=JJ-JALGT(I+1)
      IF(JT2.LT.1)JT2=1
      JF1=JJ-JALGF(I-1)
      IF(JF1.LT.1)JF1=1
      JF2=JJ-JALGF(I+1)
      IF(JF2.LT.1)JF2=1
      JF11=JF1-1
      IF(JF11.LT.1)JF11=1
      JF21=JF2-1
      IF(JF21.LT.1)JF21=1
      THET1=THETA(I-1)
      THET2=THETA(I+1)
      T11=1.-THET1
      T12=1.-THET2
C
      PR=T11*P(I-1,JF1)+THET1*P(I-1,JF11)
      VR=T11*V(I-1,JF1)+THET1*V(I-1,JF11)
      SGXR=T11*SGX(I-1,JF1)+THET1*SGX(I-1,JF11)
      UDTR=T11*UDT(I-1,JF1)+THET1*UDT(I-1,JF11)
      PS=T12*P(I2+1,JF2)+THET2*P(I2+1,JF21)
      VS=T12*V(I2+1,JF2)+THET2*V(I2+1,JF21)
      SGXS=T12*SGX(I2+1,JF2)+THET2*SGX(I2+1,JF21)
      UDTS=T12*UDT(I2+1,JF2)+THET2*UDT(I2+1,JF21)
      CP1=PR+B1*VR-C1*UDTR+GA*SGXR
```

```
      CP2=P(I-1,JT1)+B2*V(I-1,JT1)-C2*UDT(I-1,JT1)+QC*SQX(I-1,JT1)
      CM1=PS-B1*VS+C1*UDTS+QA*SQXS
      CM2=P(I2+1,JT2)-B2*V(I2+1,JT2)+C2*UDT(I2+1,JT2)+QC*SQX(I2+1,JT2)
      Q2=CP2-BC*CP1
      UDT(I1,JJ)=0.
      UDT(I2,JJ)=0.
      P(I1,JJ)=(CM2+CP2-QCA*(CM1+CP1))/(2.*QCA1)
      P(I2,JJ)=P(I1,JJ)
      V(I1,JJ)=(CP2-P(I1,JJ)*QCA1-CP1*QCA)/(B2-QCA*B1)
      V(I2,JJ)=V(I1,JJ)
      SQX(I1,JJ)=(CP1-B1*V(I1,JJ)-P(I1,JJ))/QA
      SQX(I2,JJ)=(CM1+B1*V(I2,JJ)-P(I2,JJ))/QA
      GO TO 50
C
C     INTERIOR POINTS
C
47    I1=I
      JT1=JJ-JALQT(I-1)
      IF(JT1.LT.1)JT1=1
      JT2=JJ-JALQT(I)
      IF(JT2.LT.1)JT2=1
      JF1=JJ-JALQF(I-1)
      IF(JF1.LT.1)JF1=1
      JF2=JJ-JALQF(I)
      IF(JF2.LT.1)JF2=1
      JF11=JF1-1
      IF(JF11.LT.1)JF11=1
      JF21=JF2-1
      IF(JF21.LT.1)JF21=1
      THET1=THETA(I-1)
      THET2=THETA(I)
      T11=1.-THET1
      T12=1.-THET2
C
      PR=T11*P(I-1,JF1)+THET1*P(I-1,JF11)
      VR=T11*V(I-1,JF1)+THET1*V(I-1,JF11)
      SQXR=T11*SQX(I-1,JF1)+THET1*SQX(I-1,JF11)
      UDTR=T11*UDT(I-1,JF1)+THET1*UDT(I-1,JF11)
      PS=T12*P(I+1,JF2)+THET2*P(I+1,JF21)
      VS=T12*V(I+1,JF2)+THET2*V(I+1,JF21)
      SQXS=T12*SQX(I+1,JF2)+THET2*SQX(I+1,JF21)
      UDTS=T12*UDT(I+1,JF2)+THET2*UDT(I+1,JF21)
      CP1=PR+B1*VR-C1*UDTR+QA*SQXR
      CP2=P(I-1,JT1)+B2*V(I-1,JT1)-C2*UDT(I-1,JT1)+QC*SQX(I-1,JT1)
      CM1=PS-B1*VS+C1*UDTS+QA*SQXS
      CM2=P(I+1,JT2)-B2*V(I+1,JT2)+C2*UDT(I+1,JT2)+QC*SQX(I+1,JT2)
      SQX(I1,JJ)=((CP2+CM2)/2.-(CP1+CM1)/2.)/QM
      P(I1,JJ)=(CP2+CM2)/2.-QC*SQX(I1,JJ)
      UDT(I1,JJ)=(P(I1,JJ)*(B21-1.)+CP2-B21*CP1+SQX(I1,JJ)*
     1(B21*QA-QC))/(B21*C1-C2)
      V(I1,JJ)=(CP1-P(I1,JJ)+C1*UDT(I1,JJ)-QA*SQX(I1,JJ))/B1
50    CONTINUE
C
C     VALVE
C
      IF(T.GT.TSTDY) GO TO 60
      CV=CVP
      GO TO 63
60    IF(T-TC) 61,62,62
61    TAU=(1.-SQRT(T/TC))**2
      CV=TAU*TAU*CVP
      GO TO 63
62    TAU=0.
      CV=0.
63    UDT(NPTS,JJ)=0.
      JT1=JJ-JALQT(NELM)
```

```
      IF(JT1.LT.1)JT1=1
      JF1=JJ-JALQF(NELM)
      IF(JF1.LT.1)JF1=1
      JF11=JF1-1
      IF(JF11.LT.1)JF11=1
      THET1=THETA(NELM)
      T11=1.-THET1
      PR=T11*P(NELM,JF1)+THET1*P(NELM,JF11)
      VR=T11*V(NELM,JF1)+THET1*V(NELM,JF11)
      SQXR=T11*SQX(NELM,JF1)+THET1*SQX(NELM,JF11)
      UDTR=T11*UDT(NELM,JF1)+THET1*UDT(NELM,JF11)
      CP1=PR+B1*VR-C1*UDTR+QA*SQXR
      CP2=P(NELM,JT1)+B2*V(NELM,JT1)-C2*UDT(NELM,JT1)+
     1QC*SQX(NELM,JT1)
      Z4=(CP2-QCA*CP1)/QCA1
      V(NPTS,JJ)=(-CV*Z5+SQRT((CV*Z5)**2+2.*CV*Z4))/AF
      P(NPTS,JJ)=Z4-Z5*V(NPTS,JJ)*AF
      SQX(NPTS,JJ)=(CP1-P(NPTS,JJ)-B1*V(NPTS,JJ))/QA
C
C   RESET PARAMETERS
C
      IF(JJ.LT.NSFT2)RETURN
      IF(JJ/NSFT*NSFT.EQ.JJ) GO TO 69
      RETURN
69    DO 70 I=1,NPTS
      DO 70 J=1,NSFT
      P(I,J)=P(I,J+NSFT)
      V(I,J)=V(I,J+NSFT)
      SQX(I,J)=SQX(I,J+NSFT)
70    UDT(I,J)=UDT(I,J+NSFT)
      JJ=JJ-NSFT
      RETURN
      END
C*********************************************************************
      SUBROUTINE PRINT
      COMMON/PASS/JJ,T,SK(4),SM(4),SC(4)
      COMMON/P/P(15,50),V(15,50),SQX(15,50),UDT(15,50),
     1XL(15),NTYP(15)
      COMMON/CONST/PI,XLMIN,PRES,S,TMAX,TC,DT,KOUNT,KPLOT,NSTDY,
     1ND,NELM,NELBW,IP1,IP2,IP3,IU1,IU2,J1,J2,J3,J4,J5,PJOUK
      IF(T.GT.0)GO TO 10
      WRITE(7,1)
1     FORMAT(4X,'***PRINT AND PLOT DATA***',/,4X,'INPUT KOUNT
     1(PRINT DATA INCREMENT)',$)
      READ(5,*)KOUNT
      WRITE(1,100)KOUNT
100   FORMAT(/,4X,'KOUNT= ',I5)
      WRITE(7,2)
      WRITE(1,2)
2     FORMAT(4X,'INPUT 5 POINTS FOR PRINTOUT INFORMATION')
      READ(5,*)J1,J2,J3,J4,J5
      WRITE(1,110)J1,J2,J3,J4,J5
110   FORMAT(4X,5I5)
      WRITE(7,3)
3     FORMAT(4X,'INPUT KPLOT(PLOT DATA INCREMENT)',/4X,'IF NO PLOTS
     1 ARE WANTED, KPLOT=0',2X,$)
      READ(5,*)KPLOT
      IF(KPLOT.EQ.0)GO TO 10
      WRITE(7,4)
      WRITE(1,4)
4     FORMAT(4X,'INPUT 3 POINTS FOR PRESSURE PLOTS, AND 2
     1POINTS FOR ELBOW VELOCITY PLOTS',/)
      READ(5,*)IP1,IP2,IP3,IU1,IU2
      WRITE(1,130)IP1,IP2,IP3,IU1,IU2
130   FORMAT(4X,5I5)
10    WRITE(7,20)T/S
```

```
      WRITE(1,20)T/S
20    FORMAT(/4X,'TIME=',F10.3,'MS')
      WRITE(7,30)P(J1,JJ)*S,P(J2,JJ)*S,P(J3,JJ)*S,P(J4,JJ)*S,
     1P(J5,JJ)*S,V(J1,JJ),V(J2,JJ),V(J3,JJ),V(J4,JJ),V(J5,JJ),
     1SGX(J1,JJ)*S,SGX(J2,JJ)*S,SGX(J3,JJ)*S,SGX(J4,JJ)*S,
     1SGX(J5,JJ)*S,UDT(J1,JJ),UDT(J2,JJ),UDT(J3,JJ),UDT(J4,JJ),
     1UDT(J5,JJ)
      WRITE(1,30)P(J1,JJ)*S,P(J2,JJ)*S,P(J3,JJ)*S,P(J4,JJ)*S,
     1P(J5,JJ)*S,V(J1,JJ),V(J2,JJ),V(J3,JJ),V(J4,JJ),V(J5,JJ),
     1SGX(J1,JJ)*S,SGX(J2,JJ)*S,SGX(J3,JJ)*S,SGX(J4,JJ)*S,
     1SGX(J5,JJ)*S,UDT(J1,JJ),UDT(J2,JJ),UDT(J3,JJ),UDT(J4,JJ),
     1UDT(J5,JJ)
30    FORMAT(/,(5E12.3))
      RETURN
      END
C*************************************************************************
      SUBROUTINE PLOT
      COMMON/PLOT/TPLT(200),UPLT(2,200),PPLT(3,200),KK
      LOGICAL*1 FNAME(15)
C
C     ELBOW VELOCITY PLOTS
C
190   WRITE(7,200)
200   FORMAT(' DO YOU WANT ELBOW VELOCITY PLOTS(Y/N)?',$)
      READ(5,210)IU
210   FORMAT(A1)
      IF(IU.NE.1HY) GO TO 290
      DO 270 I=1,2
      CALL GTLIN(FNAME,' ENTER UDOT FILENAME')
      OPEN(UNIT=1,NAME=FNAME,TYPE='NEW')
      WRITE(1,220)
220   FORMAT(' ;  UDOT FILE')
      DO 250 J=1,KK
      WRITE(1,240) TPLT(J),UPLT(I,J)
240   FORMAT('RD',2G15.7)
250   CONTINUE
      WRITE(1,260)
260   FORMAT('ED')
      CLOSE(UNIT=1)
270   CONTINUE
C
C     PRESSURE PLOTS
C
290   WRITE(7,300)
300   FORMAT(' DO YOU WANT PRESSURE PLOTS(Y/N)?',$)
      READ(5,210)IPR
      IF(IPR.NE.1HY) GO TO 999
      DO 380 I=1,3
      CALL GTLIN(FNAME,' ENTER PRESS FILENAME')
      OPEN(UNIT=1,NAME=FNAME,TYPE='NEW')
      WRITE(1,320)
320   FORMAT(' ;  P FILE')
      DO 360 J=1,KK
      WRITE(1,350) TPLT(J),PPLT(I,J)
350   FORMAT('RD',2G15.7)
360   CONTINUE
      WRITE(1,370)
370   FORMAT('ED')
      CLOSE(UNIT=1)
380   CONTINUE
999   CONTINUE
      RETURN
      END
```

LIST OF REFERENCES

LIST OF REFERENCES

1. Joukowsky, N. E., translated by O. Simin as "Water Hammer," Proceedings, American Water Works Association, Vol. 24, 1904, pp. 341-424.

2. Wylie, E. B., Streeter, V. L., Fluid Transients, McGraw-Hill, 1978.

3. Chaudhry, M. H., Applied Hydraulic Transients, Van Nostrand Reinhold Co., 1976.

4. Skalak, R., "An Extension of the Theory of Water Hammer," Trans. ASME, Vol. 78, No. 1, 1956, pp. 105-116.

5. Thorley, A. R. D., "Pressure Transients in Hydraulic Pipelines," ASME Journal of Basic Engineering, Vol. 91, Sept. 1969, pp. 453-461.

6. Williams, D. J., "Waterhammer in Non-Rigid Pipes: Precursor Waves and Mechanical Damping," Journal of Mechanical Engineering Science, Institute of Mechanical Engineers, Vol. 19, No. 6, 1977, pp. 237-242.

7. Walker, J. S., Phillips, J. W., "Pulse Propagation in Fluid Filled Tubes," Journal of Applied Mech., Trans. ASME, March 1977, pp. 31-35.

8. Lin, T. C., and Morgan, G. W., "Wave Propagation Through Fluid Contained in a Cylindrical, Elastic Shell," Journal of Acoustical Society of America, Vol. 28(6), 1956, pp.1165-1173.

9. Blade, R. J., Lewis, W., and Goodykoontz, J. H., "Study of a Sinusoidally Perturbed Flow in a Line Including a 90 deg Elbow with Flexible Supports," NASA Technical Note D-1216, 1962.

10. Wood, D. J., "A study of the Response of Coupled Liquid Flow-Structure Systems Subjected to Periodic Disturbances," Jour. of Basic Engr., Trans. ASME, Vol. 90, Dec. 1968, pp. 532-540.

11. Davidson, L. C., and Smith, J. E.,"Liquid-Structure Coupling in Curved Pipes," The Shock and Vibration Bulletin, No. 40, Part 4, Dec. 1969, pp. 197-207.

12. Davidson, L. C., and Samsury, D. R. ,"Liquid-Structure Coupling in Curved Pipes-II," The Shock and Vibration Bulletin, No. 42, Part 1, Jan. 1972, pp. 123-125.

13. Hatfield, F. J., Wiggert, D. C., and Otwell, R. S., "Fluid-Structure Interaction in Piping by Component Synthesis," ASME Journal of Fluids Engineering, Vol. 104, No. 4, Sept. 1982, pp. 318-325.

14. Hatfield, F. J., Davidson, L. C., and Wiggert, D. C.,"Acoustic Analysis of Liquid-Filled Piping by Component Synthesis: Experimental Validation and Examination of Assumptions," Fluid Transients and Fluid-Structure Interaction, ASME PVP-Vol. 64, 1982, pp. 106-115.

15. Phillips, J. W.,"Reflection and Transmission of Fluid Transients at Elbows," TAM Report No. 425, University of Illinois at Urbana-Champaign, May 1978.

16. Wood, D. J., "Influence of Line Motion on Waterhammer Pressures," Journal of Hydraulics Division, Proc. ASCE, Vol. 95, May 1969, pp. 941-959.

17. Wood, D. J., and Chao, S. P., "Effect of Pipeline Junctions on Waterhammer Surges," Transportation Engineering Journal, Proc. ASCE, Vol. 97, Aug. 1971, pp. 441-456.

18. Ellis, J., "A Study of Pipe-Liquid Interaction Following Pump Trip and Check-Valve Closure in a Piping Station," Proc. Third Intl. Conf. on Pressure Surges, Vol. 1, BHRA Fluid Engr., Canterbury, England, March 1980, pp. 203-220.

19. Schwirian, R. E., and Karabin, M. E., "Use of Spar Elements to Simulate Fluid-Solid Interaction in the Finite Element Analysis of Piping System Dynamics," Symposium on Fluid Transients and Structural Interactions in Piping Systems, ASME, June 1981, pp. 1-11.

20. Giesecke, H. D., "Calculations of Piping Response to Fluid Transients Including Effects of Fluid/Structure Interaction," Sixth International Conference on Structural Mechanics in Reactor Technology, North-Holland Publishing Co., August 1981.

21. Otwell, R. S., "The Effect of Elbow Translations on Pressure Transient Analysis of Piping Systems," Fluid Transients and Fluid-Structure Interaction, ASME PVP-Vol. 64, 1982, pp. 127-136.

22. Wiggert, D. C., and Hatfield, F. J. "Time Domain Analysis of Fluid-Structure Interaction in Multi-Degree-of Freedom Piping System," Proc. 4th Intl. Conf. on Pressure Surges, BHRA, Sept. 1983.

23. Swaffield, J. A. "The Influence of Bends On Fluid Transients Propagated in Incompressible Pipe Flow," Proc. Inst. Mechnical Engrs., Vol. 183, Pt. 1,No. 29, 1968-69, pp. 603-614.

24. Forsythe, G. E., and Wasow, W. R., Finite Difference Methods for Partial Differential Equations, John Wiley and Sons, Inc. 1960.

25. Craig, R. R., Structural Dynamics, John Wiley & Sons, 1981.

26. White, R. N., Gergely, P., Sexsmith, R. G., Structural Engineering, John Wiley & Sons, 1976